

Systemic Skeletal Diseases

S. Waldt, D. Müller, T. Link

38.1 Congenital Sclerotic Skeletal Diseases – 1042

38.2 Acquired Sclerosing Bone Diseases – 1044

38.3 Metabolic Bone Diseases – 1046

38.3.1 Osteoporosis (General) – 1046

38.3.2 Types of Osteoporosis – 1053

38.3.3 Osteomalacia – 1055

38.3.4 Hyperparathyroidism – 1057

38.3.5 Renal Osteopathy – 1058

38.3.6 Hypoparathyroidism – 1059

38.3.7 Pseudohypoparathyroidism – 1060

38.3.8 Osteopathies in Hypo-/Hypervitaminosis – 1060

38.3.9 Endocrine Bone Diseases – 1061

38.3.10 Bone Diseases caused by Toxicity – 1062

38.4 Osteonecrosis and Bone Infarction – 1063

38.4.1 Osteonecrosis in Adults – 1063

38.4.2 Osteonecrosis in Children and Adolescents – 1066

38.4.3 Bone Infarction – 1069

38.5 Bone Changes in Diseases of Haematopoietic and Reticulohistiocytic Systems – 1070

38.5.1 Anaemia – 1070

38.5.2 Myeloproliferative Diseases and Leukaemias – 1072

38.5.3 Diseases of Reticulohistiocytic Systems – 1074

38.6 Systemic Osteoarthropathies – 1075

38.6.1 Phakomatoses – 1075

38.6.2 Amyloidosis – 1076

38.6.3 Sarcoidosis – 1077

Bibliography – 1077

38.1 Congenital Sclerotic Skeletal Diseases

S. Waldt

■ Osteopoikilosis

■ Definition

Osteopoikilosis is a rare and benign disease characterised by multiple round osteosclerotic lesions throughout the whole skeletal system.

■ Clinical Presentation

Osteopoikilosis is asymptomatic and is usually found incidentally. In ca. 10–25% of cases, the disease is associated with various skin lesions. An autosomal dominant inheritance can be assumed based on family examinations. Osteosclerotic lesions show histological similarities to bone islands and osteoma (▶ Chap. 36).

■ Imaging

The **radiographic appearance** is pathognomonic: mostly periarticular, meta- and epiphyseal, multiple, round, or ovoid foci of sclerosis (■ Fig. 38.1). Predilection sites are the long tubular bones. Occurrences in the carpal and tarsal bones, pelvis, and scapula are also common. Although most lesions are constant over the course of time, they can also be dynamic, which means increasing or decreasing in size and number. As a rule lesions exhibit no increased activity on scintigraphy.

Differential diagnosis considerations include osteoblastic metastases, mastocytosis, and tuberous sclerosis. Usually the symmetric distribution, the periarticular location, and the typical morphology of lesions as well as the missing clinical symptoms allow for the correct diagnosis. Therefore, in most cases apart from conventional radiographs no additional imaging modalities are necessary. In doubtful cases particularly a normal bone scan may support the diagnosis.

■ Osteopathia Striata

■ Definition

Synonym: Voorhoeve disease.

Osteopathia striata is a very rare hyperostotic osteopathy that is characterised by striped, ribbon-like bands of osteosclerosis that extend from the diaphyses into the metaphyses of long tubular bones.

■ Clinical Presentation, Epidemiology, and Aetiology

Similar to osteopoikilosis, osteopathia striata is usually asymptomatic. It originates from an autosomal dominant inheritance. Men and women are equally affected.

■ Imaging

Radiography reveals linear and ribbon-like sclerosis extending predominantly from the diaphysis into the metaphysis of long tubular bones but sometimes with extension into the epiphysis (■ Fig. 38.2). Changes are usually bilateral.

Osteopathia striata is frequently associated with other bone diseases, such as osteopoikilosis, melorheostosis, and osteopetrosis. **Differential diagnosis** considerations include vertical



■ Fig. 38.1 Osteopoikilosis. AP radiograph shows multiple round and ovoid sclerotic foci with predominantly periarticular location in the distal femur, proximal tibia, and fibula



■ Fig. 38.2 Osteopathia striata. AP radiograph of the pelvis demonstrates linear and ribbon-like sclerotic lesions in the metaphysis and diaphysis of both femora that reach up to the epiphysis. In addition, related bilateral changes are delineated in the superior and inferior pubic ramus

sclerotic lines that appear as normal variants, the adult form of osteopetrosis, and the less common Ollier disease, which along with enchondroma also demonstrates linear metaphyseal thickening. Because of an overall characteristic radiographic appearance, no additional imaging modality is necessary apart from radiography.

■ Melorheostosis

■ Definition

Synonym: Osteosis eburnisans monomelia.

Melorheostosis is an acquired mesodermal disorder with epiosteal, endosteal, and soft-tissue bone formation with typical segmental occurrence in the long tubular bones, mostly of the lower extremities. The “candle wax flowing” appearance of cortical hyperostosis is a characteristic appearance in radiologic imaging.

■ Clinical Presentation, Pathogenesis

Pain caused by the soft tissue changes, which are associated with the skeletal changes, is present in the affected extremities. Osseous findings of melorheostosis are generally asymptomatic, but fibrovascular formations in the medullary space may occasionally lead to an increase of intraosseous pressure and pain.

Histology of newly formed bone shows a lamellar bone structure, and the trabeculae can have sclerotic thickening with irregularly organised Haversian canals. Soft tissue changes are caused by fibrous cartilage islands with endochondral ossification and muscle changes with myositis and mysclerosis.

■ Imaging

The **radiographic appearance** is highly characteristic with longitudinal, ribbon-like hyperostosis that resembles “flowing candle wax” (■ Fig. 38.3). This hyperostosis produces thickening of the cortical bone with an irregular, wavy, or sometimes lobulated contour of the affected bone. Endosteal hyperostosis leads to inner-lying longitudinal bone formation that warps up against the medullary cavity. The formation of new bone tends to have an eccentric location, which means only one side of the bone is affected. Radiologic diagnosis can be made sufficiently with conventional radiographs. In evidence of melorheostotic changes, the whole affected extremity should be examined with conventional radiography.

In cases with stronger clinical symptoms, **MRI** should be performed in order to determine soft tissue changes.

Differential diagnosis considerations vary because hyperostotic changes in melorheostosis occur in different locations and with different grades of severity. The long and smoothly contoured hyperostosis of long bones must be differentiated from osteomas and osteoid osteomas, whereas the wavy and irregularly configured cortical and juxtacortical hyperostosis, as well as periarticular nodular and conglomerate-like hyperostosis, must be differentiated from juxtacortical osteosarcoma and from changes associated with myositis ossificans.

■ Mixed Sclerosing Bone Dystrophy

Mixed sclerotic bone dystrophy is a disease that involves two or all three of the diseases osteopoikilosis, osteopathic striata, and melorheostosis.

■ Pachydermoperiostosis

■ Definition

Synonyms: primary hypertrophic osteoarthropathy, Touraine-Solente-Golé syndrome.



■ Fig. 38.3a,b Melorheostosis. Conventional radiographs of the lower leg (a AP and b lateral view) reveal pronounced lateroventral hyperostosis of the proximal tibia that resembles “flowing candle wax.” The outer contour of the new bone formation is wavy and lobular. In this case, only a mild endosteal component of hyperostosis is evident

Idiopathic pachydermoperiostosis is an autosomal dominant hereditary disorder that is characterised by thickening of the skin (pachydermia) and the periosteum of short and long tubular bones. It is very rare. The primary hereditary form accounts for 3–5% of all cases of hypertrophic osteoarthropathy.

■ Pathogenesis, Clinical Presentation

Pachydermoperiostosis typically begins in adolescence and shows different patterns of appearance depending on the severity (“form fruste” up to presentation of the full syndrome). Characteristic signs include changes to the cutis and subcutis with characteristic coarsening of the face and scalp, thickening of the lower arms and legs, paw-like appearance of hands and feet. Periosteal reactions are present as well as arthralgia, synovitis, clubbed fingers and toes, and vegetative nervous system dysregulations.

■ Imaging

Periosteal proliferations resulting in osseous appositions with irregular and sometimes blurry contours stand out the most in radiologic examination. This occurs first and foremost in the diaphysis of short and long tubular bones and, in contrast

to secondary hypertrophic osteoarthropathy, can extend to the epiphysis. Ossification of the joint capsule, tendons, and especially smaller joints can occur in the course of the disease. Pelvic involvement is rare, yet cases have been reported. Osteolysis of the distal phalanges can occur in advanced cases.

The most important **differential diagnosis** considerations of pachydermoperiostosis include secondary hypertrophic osteoarthropathy and thyroid acropachy. Nevertheless, both of these diseases are relatively easy to distinguish from pachydermoperiostosis due to their different clinical presentations and appearances in imaging.

38.2 Acquired Sclerosing Bone Diseases

S. Waldt

■ Secondary Hypertrophic Osteoarthropathy

■ ■ Definition

Synonyms: Pierre-Marie-Bamberger syndrome, symptomatic pachydermoperiostosis.

Pierre-Marie-Bamberger syndrome mostly has an underlying cause of intrathoracic neoplastic disease and is characterised by the secondary occurrence of bilateral periosteal bone reactions in the diaphysis and metaphysis of short and long tubular bones, clubbed fingers, arthralgia, and arthritic symptoms.

■ ■ Pathogenesis

Neoplastic intrathoracic diseases are usually an underlying cause of secondary hypertrophic osteoarthropathy, for example bronchial carcinoma (>90% of cases), lung metastases, mesothelioma, or Hodgkin's disease. In addition, non-neoplastic diseases, for example chronic pleuropulmonary diseases, cyanotic heart failure, or gastrointestinal diseases, can lead to secondary hypertrophic osteoarthropathy in rare cases.

■ ■ Clinical Presentation

Secondary hypertrophic osteoarthropathy is characterised by the following basic features: clubbed fingers with shiny or glossy nails, hyperhidrosis of the hands and soles of feet, arthralgia, and arthritic findings.

■ ■ Imaging

Periosteal appositions are the main characteristic feature in imaging; these usually have bilateral occurrence in the proximal diaphysis of short and long tubular bones. Commonly affected long bones are mostly the tibiae, fibulae, radii, and ulnae; less commonly affected are the femora, humeri, metacarpals, and metatarsals. In the course of the disease the diaphyseal periosteal changes frequently extend into the metaphysis while the epiphysis characteristically is spared. Linear periosteal appositions are typical and are delineated against the cortex by a lower density.

■ Hyperostosis Frontalis Interna

Hyperostosis frontalis interna is a thickening of the frontal diploë originating from the tabula interna by the apposition of bone.

Imaging. Hyperostosis frontalis interna is usually discovered incidentally and without clinical relevance. It is found predominantly in women of older age. Conventional radiography and CT reveal characteristic findings of a symmetric, mostly cloudy thickening of the inner table of frontal bone, where osseous changes can also affect the parietal bone (■ Fig. 38.4).

■ Infantile Cortical Hyperostosis

Synonym: Caffey disease.

Infantile cortical hyperostosis is a rare disease of unclear aetiology. It develops in the first month of life accompanied by fever and pronounced soft tissue swelling and is caused by pronounced periosteal bone apposition to cortical hyperostosis. Main manifestation sites are the mandibula, ribs, clavicle, and the short and long tubular bones, though epiphyseal portions of long bones are spared. In most cases symptoms spontaneously resolve within 6–12 months.

■ Chronic Venous Insufficiency

Chronic venous insufficiency involves bilateral periosteal reactions in the long bones of the lower extremities.

Typical symptoms of chronic venous insufficiency are lower leg oedema, skin discoloration, and foot ulcers in more advanced stages.

Imaging. The following **radiographic appearance** is characteristic:

- Pronounced cortical thickening via periosteal bone apposition in the metaphysis and diaphysis of short and long tubular bones; the periosteal bone formations produce an undulating contour of the tubular bones
- Appositioned new bone formation is typically somewhat more radiolucent than the original cortex; in primary hypertrophic osteoarthropathy and thyroid acropachy, periosteal bone appositions are typically not delineated from the cortical bone

■ Diffuse Idiopathic Skeletal Hyperostosis (DISH)

■ ■ Definition

Synonyms: Forestier's disease, spondylosis hyperostotica, ankylosing hyperostosis.

Diffuse idiopathic skeletal hyperostosis describes a disease characterised by confluent bony appositions of the anterior vertebral surfaces, formation of hyperostotic spondylophytes, and ossification of spinal ligaments and joint capsules of the zygapophyseal joints caused by osteoplastic diathesis (osseous metaplasia of fibrous tissue).

■ ■ Epidemiology, Clinical Presentation

Aetiology of diffuse idiopathic skeletal hyperostosis is unclear. Occurrence is common in older patients in the second half of life.



■ **Fig. 38.4a,b** Hyperostosis frontalis interna. **a** Lateral radiograph of the skull shows hyperostosis of the tabula interna of the frontal squama. **b** Transverse CT image of another patient more clearly demonstrates thickening of the diploë and nodular hyperostosis of the frontal bones

Men are somewhat more frequently affected than women. Symptoms are generally mild compared to radiographic changes. Typical symptoms include chronic back pain which may last for years.

■ ■ Imaging

Resnick outlines three criteria for the diagnosis of spinal DISH:

- Evidence of confluent (sugar-pouring) calcification and ossification ventrolateral of at least four contiguous vertebrae.
- The height of the intervertebral disc space must be preserved, and there must be no relevant findings of osteochondrosis in the affected segments (marginal osteophytes, vacuum phenomenon etc.)
- The zygapophyseal joints do not show ankylosis and the sacroiliac joints must not show erosive changes, sclerosis, and ankylosis.



■ **Fig. 38.5** Diffuse idiopathic skeletal hyperostosis (DISH). Lateral radiograph of the thoracic spine shows confluent hyperostotic ossifications at the anterior surfaces of middle and lower thoracic vertebrae expanding over five contiguous vertebrae. There are no relevant findings of osteochondrosis in the affected segments

Resnick formulated these criteria in order to differentiate DISH from degenerative spine disease.

Radiographic findings in different manifestation sites of DISH include:

- **Thoracic and lumbar spine:** calcification and ossification along the ventrolateral aspect of the vertebral bodies with prominence in the lower thoracic and upper lumbar spine; on the lateral aspect of the thoracic spine, ossification is more prominent on the right than on the left due to aortic pulsations (■ Fig. 38.5)
- Calcifications, particularly in the periphery of the intervertebral discs
- **Cervical spine:** focus of osseous appositions in the lower cervical spine (C4–7); ossification of the posterior longitudinal ligament can lead to spinal stenosis
- **Pelvis:** ligament and tendon calcification/ossification at the iliac crest, the ischial tuberosity, and the trochanters; ossification of the iliolumbar and sacrotuberous ligaments; heterotopic ossification following implantation of TEP are usually more prominent than in the normal population
- **Calcaneus:** plantar and dorsal calcaneal spurs; thickening of plantar and dorsal cortex of the calcaneus
- Calcification of ligamentous and tendinous insertions are also common in the **knee, elbow, and shoulder**

38.3 Metabolic Bone Diseases

D. Müller, T. Link

38.3.1 Osteoporosis (General)

■ Basics

■ ■ Definition

Osteoporosis is a metabolic bone disease defined by low bone mass and deterioration of trabecular bone structure which consequently leads to an elevated risk of fracture.

The WHO (1994) defines osteoporosis by measurement of “bone mineral density” (BMD). A BMD >2.5 standard deviation below the mean peak bone mass (average of young, healthy population) (T score = <2.5) defines **osteoporosis**. A BMD of 1–2.5 standard deviation below the average (T score = -1 to -2.5) indicates **osteopaenia**. These definitions are based on “dual-energy X-ray absorptiometry” (DXA), a measurement used for cases involving the spine (AP or PA measurement), proximal femur, and the distal radius (■ Table 38.1). The standard deviation applies to postmenopausal women but not to men or women of younger age.

In 2000 this definition, which was established at the **NIH Consensus Development Conference** in 1993, was modified. The term osteoporosis was thereby defined as a skeletal disease defined by reduced bone strength, which in turn leads to the elevated risk of fracture. For a more precise formulation, the following was added: bone strength is characterised by two main characteris-

■ Table 38.1 WHO classification of degrees of osteoporosis by T-score

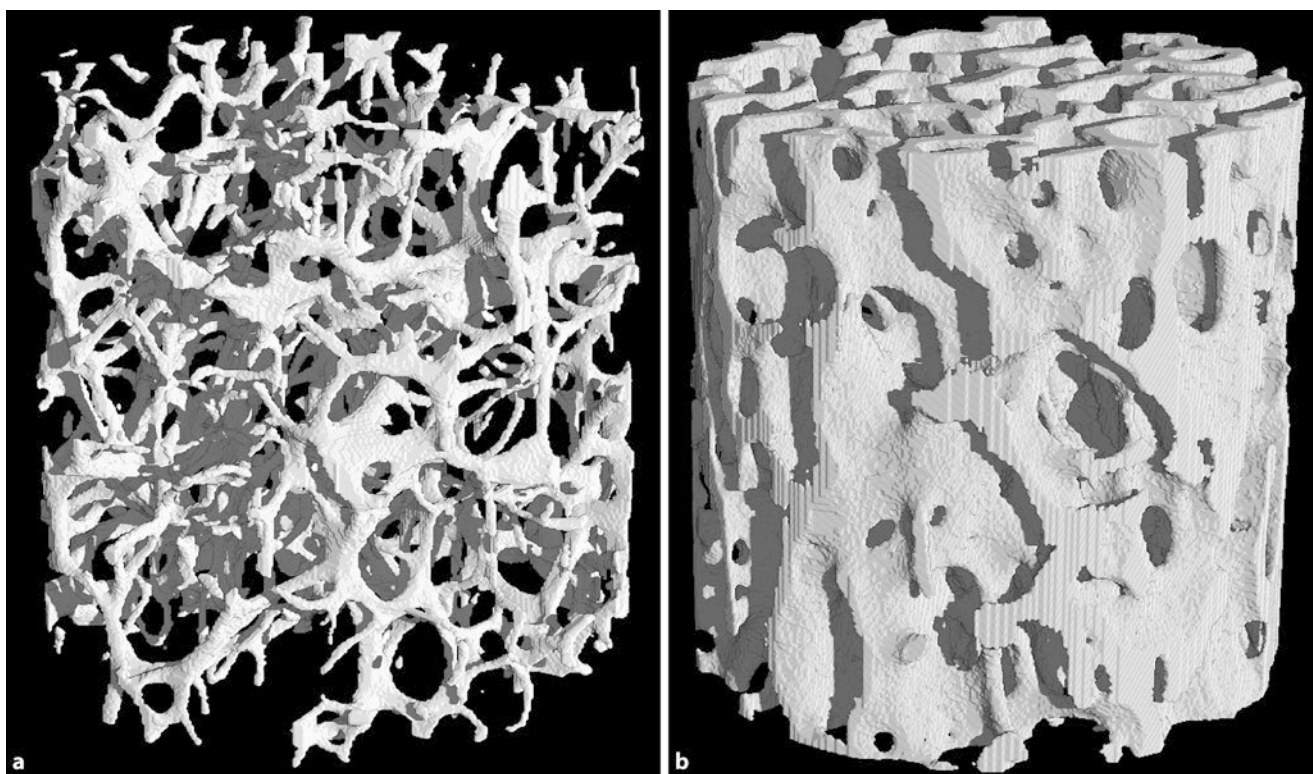
T-Score	Diagnosis
T-Score >-1	Normal
$-2.5 < \text{T-Score} < -1$	Osteopaenia
T-Score <-2.5	Osteoporosis
T-Score <-2.5 and Fractures	Manifest osteoporosis

tics: **bone density and bone quality**. In this case, bone density is measured by mineralisation per surface or volume. Whereas bone density is dependent on the peak bone mass and the amount of bone loss, bone quality, on the other hand, is determined by architecture, microinjuries, and mineralisation (■ Fig. 38.6).

■ ■ Pathophysiology

The pathophysiology of osteoporosis is determined by an insufficiency of osteoblasts and increased activity of osteoclasts. In addition, cancellous bone, which consists of a network of plate-like trabecular bone, is affected. This trabecular microarchitecture plays a determining role in the mechanical weight-bearing capacity of bone.

“Bone resorption” in trabecular bone is a physiologic condition. If the lacunae are abnormally deep, the trabeculae can separate, which is also known as **perforation**. Osteoclasts, or “killer osteoclasts,” cause this. Because osteoblasts are unable to repair



■ Fig. 38.6a,b μCT of trabecular bone structure of the distal radius. a Osteoporotic bone. b Normal bone. Healthy trabecular bone demonstrates trabecular bone thickness with small medullary spaces. In contrast, osteopo-

rotic bone demonstrates expanded perforation of the trabecular structure with noticeably expanded medullary spaces

this damage, a so-called “uncoupling” of affected trabeculae occurs. Although perforations are only accompanied by a mild loss of bone density, they reveal noticeable disruption of the trabecular microarchitecture.

Another important factor for stability of cancellous bone is the so-called **microcallus formations**, which can be observed in areas of maximum mechanical stress without trauma.

■ ■ Aetiology

Aetiology of osteoporosis is classified into two categories as shown below.

Primary Osteoporosis. This is the most common form with a frequency of 95%. It is subdivided further into:

- Idiopathic osteoporosis, uncommon and occurring in young patients
- Postmenopausal osteoporosis (type 1 osteoporosis)
- Senile osteoporosis (type 2 osteoporosis)

Postmenopausal osteoporosis has two phases, where at the beginning the “fast-looser” patients are prevalent. The loss of bone density accounts for a high turnover rate of $> 3.5\%$ per year. After about 10 years, the loss of trabecular bone decreases to a low turnover of $< 3.5\%$ per year. Postmenopausal osteoporosis mostly affects the vertebral cancellous bone and occurs almost exclusively in women after the age of 50; its aetiology is defined by a deficit of oestrogen.

In contrast to postmenopausal osteoporosis, **senile osteoporosis** affects compact bone. It manifests in fractures involving the femoral neck, humerus, radius, and vertebrae. Women are twice more affected than men. Its pathophysiological causes are the general aging process, lack of physical activity, and eventual deficit of calcium and/or vitamin D.

Secondary Osteoporosis. Secondary osteoporosis, with an occurrence of only about 5%, has different aetiologies. These include endocrine diseases such as hypercortisolism, hypogonadism, hyperthyroidism, hyperparathyroidism, and osteomalacia etc. It can be evident in cases with symptoms of malabsorption with limited supply of/resorption of calcium or vitamin D, for example in gastrointestinal diseases such as Crohn’s disease, ulcerative colitis, primary biliary cirrhosis, or anorexia. Moreover, immobilisation and iatrogenic/medicamentously induced osteoporosis should be considered as a possible cause.

The latter term applies to long-term therapy with heparin, methotrexate, an anticonvulsant, or cortisol. Osteoporotic side effects must be assumed with daily intake of a substance equivalent to $> 5\text{--}7.5$ mg prednisolone for over three months, and prophylactic medication for osteoporosis is recommended after 6 months in the steroid dosage mentioned above. The osteoporotic effects of glucocorticoids are caused by changes in intestinal calcium absorption, renal calcium excretion, vitamin D and parathormone metabolism, gonad function, and last but not least, an imbalance of osteoblasts and osteoclasts.

In contrast to hereditary diseases like Ehlers–Danlos syndrome, Marfan syndrome, homocystinuria, or osteogenesis imperfecta, the relation to other diseases associated with osteoporo-

sis remains unclear, for example rheumatoid arthritis and other autoimmune diseases.

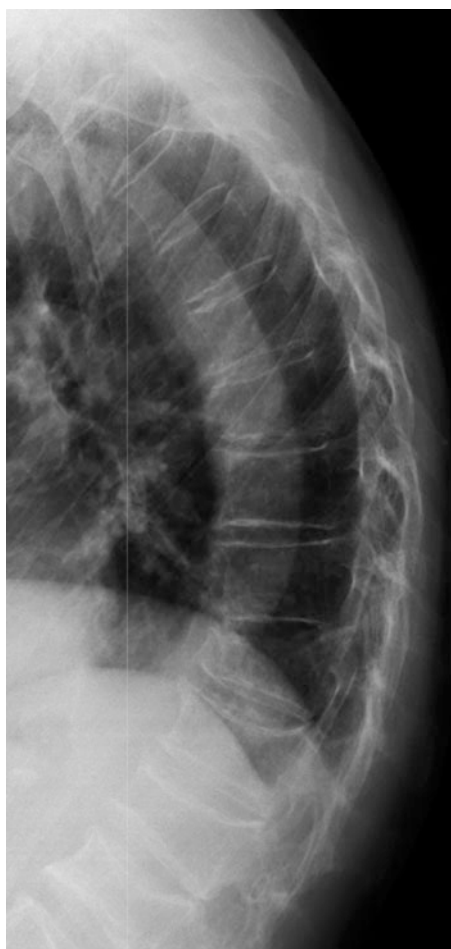
■ Examination Techniques and Results

■ ■ Imaging: Spine

➤ **Conventional X-ray diagnosis is not a suitable method for early detection of osteoporosis.**

Osteoporosis is only detectable using conventional X-ray images after a 20–40% rate of demineralisation has occurred. Furthermore, the common radiologic signs of osteoporosis, such as increased radiolucency, a rarefied spongiosa appearance, prominence of vertebral end and base plates and cortical thinness, are unreliable. In contrast to this, compression fractures in the spine are a reliable late sign of manifested osteoporosis (■ Fig. 38.7).

The **analysis of spinal deformities** plays an important role in diagnosis as well as in the course of the disease. An osteoporotic spinal deformity occurs in women > 50 years of age with a frequency of up to 25%. Spinal deformities contribute significantly to the risk of additional osteoporotic fractures. Diagnosis



■ Fig. 38.7 **Osteoporosis of the thoracic spine.** Demineralised thoracic spine with pronounced base- and endplates and typical osteoporotic vertebral deformities of the mid thoracic spine and thoracolumbar junction

Table 38.2 Semiquantitative indices for determination of grade of severity of osteoporotic vertebral deformities

Method	Classification
Spinal fracture index (SFI); Genant et al. (1993) T4 to L4	Grade 0: normal non-fractured spine Grade 1: mild fracture, anterior, central, or posterior height decrease of 20–25% Grade 2: moderate fracture, anterior, central, or posterior height decrease of 25–40% Grade 3: severe fracture, anterior, central, or posterior height decrease of > 40%
Spine deformity index (SDI); Minne et al. (1988) T5 to L4	Anterior, central, and posterior T4 height as standard. The remaining vertebrae are added up in proportion to those mentioned according to a “spine deformity index” (SDI).
Radiological vertebral index (RVI); Meunier et al. (1978) T3 to L4	1 = physiological vertebral form 2 = biconcave vertebrae 4 = wedge-shaped vertebrae, compressed vertebrae, or upper plate fracture Addition of grading, value > 20 is considered to be pathologic
Barnett–Nordin index (Barnett and Nordin 1960)	Index of quotients of central and anterior height of L3 and L4. Index < 80% should be consistent with osteoporosis. In variability of vertebral form and calculation of only two vertebral bodies, this index is of small significance.

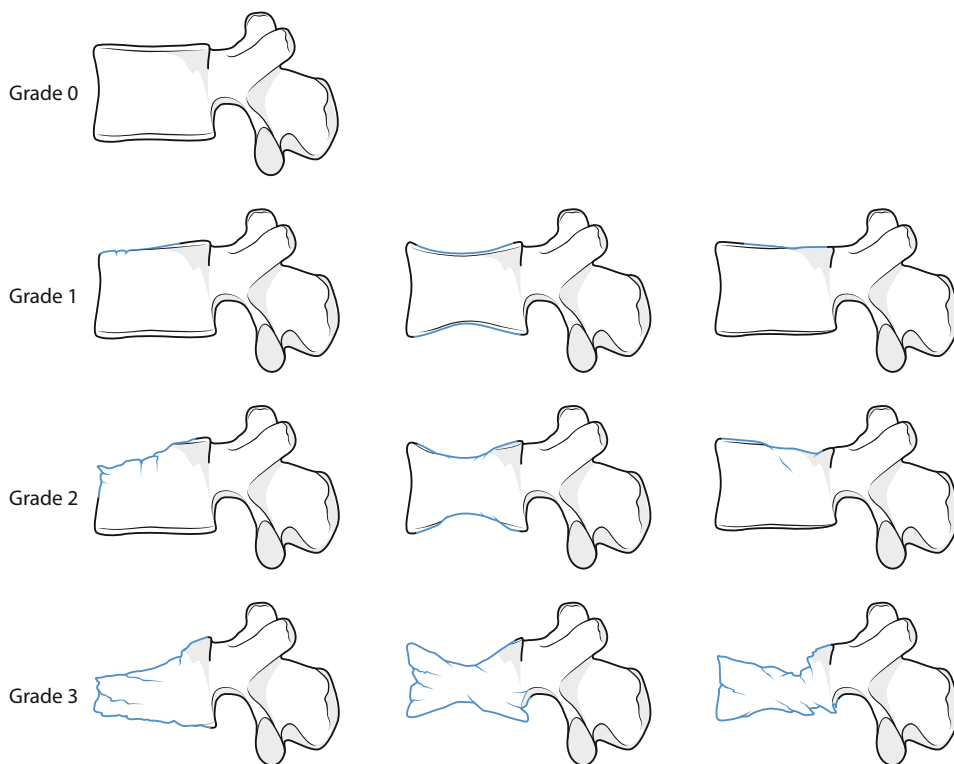


Fig. 38.8 Spinal fracture index

of osteoporotic spine fractures is generally determined by a reduction of height of at least 20% or at least 2, mostly 3, standard deviations below the mean of a normal collective population. **Table 38.2** lists the most commonly applied semiquantitative classifications (**Fig. 38.8**).

Differential Diagnosis. **Malignant diseases**, such as bone metastases and multiple myeloma, are the most important considerations in differential diagnosis.

Metastases occur ca. 50–100 times more frequently than primary bone tumours and affect the axial skeleton approx. 65% of the time. Osteolytic tumours with osseous metastasis include, first and foremost, renal cell carcinoma and thyroid carcinoma as well

as malignomas of the GI tract; osteoblastic tumours include, first and foremost, breast, prostate, and bronchial carcinoma. Breast cancer can also present as mixed osteolytic-osteoblastic lesions. Indications for metastatic occurrence are localization above T7 and deformation of the posterior spine and/or peduncle, concomitant osseous destruction, and signs of regional increase of soft tissue mass. CT or MRI is helpful for differential diagnosis (**Figs. 38.9** and **38.10**).

Multiple myeloma can appear as general osteoporosis, which traces back to the increase of “osteoclast-activating factors” (OAF). Solitary or multiple lesions as well as vertebral deformities occur in about half of all cases. In this case, MRI imaging of bone marrow enables differentiation. However, use caution



■ Fig. 38.9a,b Osteoporotic compression fracture, MRI. a STIR sequence. T8 compression fracture with corresponding endplate bone marrow oedema. b T1-weighted SE sequence shows corresponding decrease of signal intensity

when diagnosing. **Excessive haematopoiesis**, for example as in chronic lung disease, smoking or previous chemotherapy and reconversion, demonstrates a similar appearance in MRI.

Vertebral changes that occur in **osteomalacia in older patients** are similar to those in osteoporosis. The vertebrae are made up of coarse trabeculae with a faded border between medullary and cortical bone.

➤ In renal osteopathy, vertebral deformations are pathognomonic with subchondral sclerosis of ligaments and a bright central area (a so-called **Rugger-Jersey spine**).

Scheuermann's disease shows an image similar to osteoporosis of the spine. Wedge-shaped deformities occur in the vertebral endplates and a large anterior-posterior diameter becomes evident as well as a narrowing of the intervertebral space. Schmorl's nodules, defined by protrusions of intervertebral discs in subchondral weakened bone, causing growth in the form of a hunchback in opposing vertebrae (Edgren–Vaino sign), help as criteria for diagnosis.

Biconcave osteoporotic vertebrae are similar to so-called H-shaped vertebral bodies. They appear in diseases like **Gaucher's disease** or **sickle cell anaemia**.

Apart from patient medical history, post-traumatic changes, like an expanded cross-diameter of vertebrae and secondary degenerative changes, are helpful for **differentiating osteoporotic fractures from fractures caused by trauma**.

Kummel–Verneuil disease is a rare cause of spinal fracture in patients of older age. Weeks and months following spontaneous osteonecrosis of the thoracolumbar joints, unhealed small gas inclusions arise in unhealed bone fracture – the so-called vacuum phenomenon.



■ Fig. 38.10a–c Vertebral fractures, metastases. a Plain radiography, T10 and T11 vertebral fractures in a patient with known bronchial carcinoma. b Supplemental MRI STIR sequence reveals hyperintense signal alterations in the neighbouring T9 and T12 as well. c T1-weighted SE sequence consequently demonstrates a loss of fatty bone marrow signal of all vertebrae

■ ■ Imaging: Femur

In reference to mortality and morbidity, proximal femur fractures have the greatest significance of all osteoporotic fractures. This type of fracture can appear as occult in conventional X-ray radiographs; in contrast, MRI shows greater sensitivity. On this note, patients with clinical suspicion of a proximal femur fracture in nondescript X-ray should undergo a supplemental MRI examination via fat-saturated T2-weighted and native T1-weighted sequence.

Evaluation of the threat of fracture by means of conventional X-ray imaging can be made according to the **semiquantitative Singh Index**. This classification guideline looks closely at thickness and the arrangement of trabecular structures. The Singh Index defines six grades of severity; grade 1 demonstrates the highest level of rarefied trabecular bone and highest level of threat of fracture, whereas grade 6 defines the thickness of the trabecular structure as the greatest and fracture threat as the lowest.

Differential Diagnosis. Pathologic proximal femur fractures are to be considered above all else; older patients mostly present a neoplastic metastatic cause. In cases of anamnestic suspicion, supplemental MRI helps with focal signal change of fatty bone marrow that shows the character of a mass. Differential diagnosis must also consider stress and fatigue fractures.

■ ■ Diagnostic Imaging: Peripheral Skeleton

Of the peripheral skeleton, distal radius fractures present with the most difficulty. Manifestation of osteoporosis demonstrates

a typical pattern in the peripheral skeleton, especially in X-ray images of the hand. Rarefaction of the spongy structure is combined with the thinning of cortical bone from within. Intracortical and subperiosteal bone resorption must be differentiated, which are typically of osteopathies with a high bone turnover rate, for example hyperparathyroidism.

Semiquantitative modalities were developed for osteoporotic atrophy of long bones. The second metacarpal is the most evaluated bone in this case; measurements of combined cortical thickening are determined at the lateral aspect of the middle second metacarpal along with the outer and inner diameter and then compared to the measurements of a normal population.

Differential Diagnosis. Osteoporosis caused by inactivity, Sudeck's disease, and high-turnover osteopathy are considered for differential diagnosis. Hyperparathyroidism, osteomalacia, and hyperthyroidism tend to develop in bones of the hands and other extremities. In contrast, diffuse or focal neoplastic changes in the hand and foot occur rarely.

■ ■ Osteodensitometric Modalities for Diagnosis of Osteoporosis

Osteodensitometric methods are the most important means for diagnosis and quantification of osteoporosis. ■ Table 38.3 explains the differences in modalities.

The most clinically established methods are:

- Dual-energy X-ray absorptiometry (DXA)
- Quantitative CT (QCT)

■ Table 38.3 Osteodensitometric modalities for diagnosis of osteoporosis

Method	Site of measurement	Precision (%)	Reproducibility/precision (%)		Radiation exposure: dose (μSv)
DXA	Lumbar spine PA projection	4–10	1		1–50 ^b
	Lateral projection	5–15	2–6		3–50 ^b
	Proximal femur	6	1.5–3		≈ 1–2 ^c
	Whole body	3	1		≈ 3 ^c
QCT	Lumbar spine	5–15	1.5–4		60–500 ^d
Standard modality of the peripheral skeleton					
DXA	Radius	4–6	1	< 1	
pQCT	Radius	2–8	1–2	≈ 1	
Older modalities					
Dual-spectrum QCT	Lumbar spine	3–6	4–6		≈ 500 ^a
SPA/DPA	Lumbar spine	2–11	2–3		5
	Proximal femur		2–5		3
SXA	Radius/Calcaneus	4–6	1–2		> 1
Photodensitometry	Finger	10	5		< 5

^a 125 kV/85 kV and 410 mAs

^b The lowest values apply to pencil beam devices, the highest values to cone beam devices with very good image quality

^c For pencil beam devices

^d 60 μmSv is achieved by application of low-dose protocols (80 kV, 125 mAs)

DXA (Dual-Energy X-ray Absorptiometry) DXA is the most available means for measuring bone mineral density (BMD). It is based on a principle of one X-ray tube emitting X-ray beams with two different energies (kV). These are attenuated according to different tissue characteristics; bone tissue shows noticeably larger differences in the attenuation profile than soft tissue. From the difference between the attenuation profiles, a material composition can be concluded and with this one can determine an almost soft-tissue-absorption-independent bone density. For quality management, phantoms and calibration systems are integrated into the DXA measuring device.

An advantage of DXA is its high degree of precision: depending on the examined region, the error of accuracy is 1–3%, which is the highest degree of accuracy achieved in examination of the lumbar spine in PA view. With an adequate dose of 1–3 μSv , radiation exposure associated with the DXA method is very mild (Table 38.3).

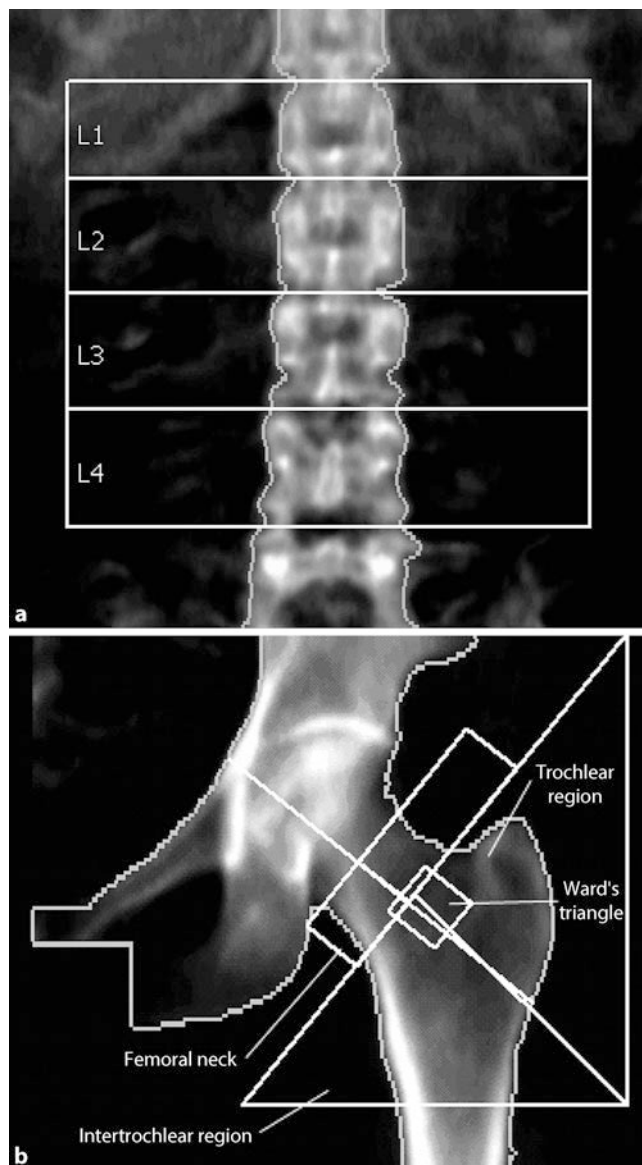
► Because of its short performance time of < 2 minutes, high reproducibility, and the low level of radiation exposure of an effective dose of 1–3 μSv , DXA has become a widely accepted method in clinical routine.

DXA of the Lumbar Spine. For examination of the lumbar spine in AP or PA view, the lower leg is elevated for minimisation of lumbar lordosis, making individual vertebrae recognisable in an automatic program for contour findings. These ROIs (regions of interest) must be controlled by the examiner in order to prevent false measurements.

BMD is generally tested by measuring L1–L4 as density/surface in g/cm^2 (Fig. 38.11). Note that the morphology of the examined region affects the acquired density. Larger vertebrae automatically have a higher BMD than smaller vertebrae without necessarily demonstrating higher volume density. An additional disadvantage of lumbar spine DXA is an overlapping effect caused by aortic sclerosis, other calcifications, and postoperative foreign bodies. Furthermore, degenerative changes such as spondylarthrosis, osteochondrosis, spondylosis, and interspinal arthrosis as well as spinal fractures and Paget's disease result in a falsely measured high BMD. Nonetheless, T-score graded DXA examination of the lumbar spine and proximal femur in AP or PA view is the **standard examination procedure in the diagnosis of osteoporosis**. The Z-score, which is a comparison value based on age and gender, is also applied, but has little significance in the diagnosis of osteoporosis.

In addition to AP or PA view DXA, lateral view DXA measurements of the lumbar spine are also taken into consideration. Although less influenced by the degeneration described above, lateral view DXA has the disadvantage that only L3 can be visualised without overlapping, resulting in weaker accuracy overall.

DXA of the Proximal Femur. DXA examination of the proximal femur helps in estimating the individual risk of the most complicated osteoporotic fractures. It requires a special, standardised positioning of the leg and reproducible evaluation software. The regions of interest (ROIs) vary from producer to producer. ROIs



► Fig. 38.11a,b Dual X-ray absorptiometry (DXA). a DXA of the lumbar spine in anteroposterior projection with corresponding ROIs in L1–L4. Measurement of a summation density, which includes, in addition to the vertebral bodies, the zygapophyseal joints, the pedicles and the spinous processes. b DXA of the left proximal femur with the corresponding ROIs

in the femoral neck, intertrochanteric region, trochanter, Ward's triangle, and the whole femur are evaluated (Fig. 38.11). Compared to the lumbar spine, it shows weaker precision. Analogous to DXA of the lumbar spine, factors that influence the elevated BMD include degenerative changes, fractures, avascular osteonecrosis, Paget's disease, and vascular as well as soft tissue calcification.

■ Quantitative Computed Tomography (QCT)

Unlike DXA, QCT measures the volume density of trabecular bone in calcium hydroxylapatite/ml. In this technique bone density is not influenced by morphologic measures, such as the diameter of the spine. Summation caused by aortic calcification

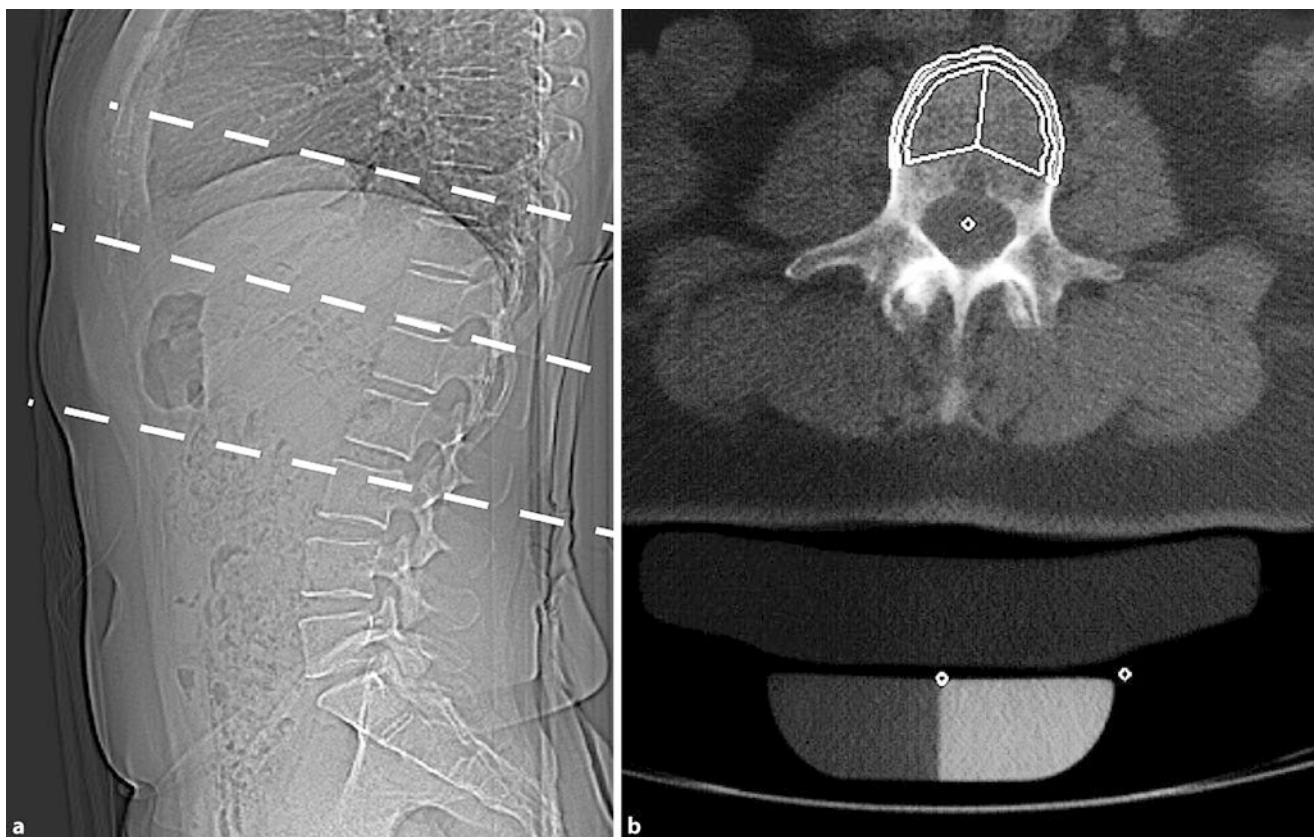


Fig. 38.12a,b Standard QCT technique. a Overview radiograph with the levels to be examined L1–L3. b Axial slice through L1 with calibration phantom and so-called “Pacman ROI” of the vertebral body

or other types of calcification and degenerative changes, such as spondylosis, spondylarthrosis and interspinal arthrosis, are avoided. However, one must take notice of vertebral pathologies that can influence bone density, for example metastasis, as well as vertebral fractures and degeneration, for example osteochondrosis.

When compared to DXA, the disadvantages to QCT include a higher dose of radiation exposure and lower degree of precision. With a radiation exposure of $60 \mu\text{Sv}$, however, it remains comparatively lower in value than the natural radiation exposure of about $2,400 \mu\text{Sv}/\text{year}$. The lower precision (2–4%) than DXA methods (1–2% for AP thoracic spine) are relativised through the isolated analysis of metabolic cancellous bone with an approximately doubled greater loss of bone density.

Examination Technique. A problem associated with QCT is the fat error, which limits accuracy. “Dual-energy QCT” (DE-QCT) was developed to correct this error. However, because accuracy is worse and radiation exposure is higher in DE-QCT than in “single energy QCT” (SE-QCT), it is SE-QCT that continues to be seen as the standard method.

The standard protocol of QCT examination consists of an analysis of L1–L3. A calibration phantom is required for conversion of Hounsfield units into milligram calcium hydroxylapatite/ml. The phantom is positioned underneath the patient’s spine and adjusted with a gel pillow to prevent air artefacts, and the lumbar lordosis is balanced out with a knee roll (■ Fig. 38.12). In an

overview radiograph (“scout view”) the morphology of the imaged spine is then evaluated. Deformed vertebrae are excluded from the analysis. Mid-vertebral cross sections with a width of 10 mm are calculated and the density of the ROIs is determined. The density of cortical and cancellous bone is automatically separately defined.

► Unlike DXA methods, T-values measured by QCT cannot be applied to the WHO definition of osteoporosis. Because of higher rates of bone density loss, noticeably more patients would be classified as osteoporotic compared to DXA methods. Along the lines of WHO criteria, Felsenberg defines a BMD of $< 80 \text{ mg/ml}$ indicative of osteoporosis and of $80\text{--}120 \text{ mg/ml}$ as indicative of osteopaenia.

In conclusion, QCT is especially suited for older patients with advanced degenerative changes of the lumbar spine. Furthermore, it is also suitable for measuring the effects of therapy, as the technique is more sensitive to the definition of cancellous bone, and for determining bone density loss in oestrogen deficiency in early menopause.

■ Peripheral Measuring Methods

In contrast to the key measuring methods described above, peripheral osteodensitometry has little significance. The disadvantages of this method include lower response rates of bone density

in peripheral bone and the limited risk approximation of spinal and femoral fractures.

Peripheral DXA. Peripheral DXA is performed at the distal radius, hand, and calcaneus. The advantages of this method include a lower radiation dose and higher precision rate in standardised ROIs. The disadvantages are, however, as mentioned, a low response of BMD and the discrepancy of T-values compared to T-values in the lumbar spine and proximal femur.

Peripheral QCT. For an analysis of peripheral volumetric bone density, special appliances have been developed, so-called “pQCT scans.” The distal radius is examined, which is suitable for diagnosis of osteoporosis due to the high percentage of cancellous bone. Along the lines of other key measuring methods, the BMD of cortical and cancellous bone can be determined separately. With such a high precision, the ultradistal radius and proximal third of the distal radius are usually measured. Advanced age leads to a simultaneous loss of cancellous bone BMD and to an increase of diameter of the radial diaphysis.

■ ■ Quantitative Ultrasound

Quantitative ultrasound (QUS) has its origin in industrial material testing. This modality only enables examination of peripheral extremities like the calcaneus, radius, or phalanges. Appliances are used with an acoustic frequency of 100 kHz to 2 MHz, which not only apply to medical imaging. In this case, clinical application measures the SOS, or “speed of sound” in m/s and the frequency-dependent attenuation of ultrasound waves (BUA = broadband ultrasound attenuation measured in dB/MHz). For BUA in patients with osteoporosis, a lower attenuation with increasing frequency is measured due to the decrease in structures of high density. In addition, SOS and BUA allow calculation of combination parameters, for example calculation of bone rigidity, which shows better reproducibility.

QUS is best suited for the examination of the calcaneus. This measurement is best made with a water bath system or using ultrasound gel.

Compared to DXA and QCT, the **advantages** of QUS include easy usability, the portable and affordable appliances, and the fact that the patient is not exposed to radiation. An assurance of quality of QUS in daily, software-supported testing is observed.

■ ■ Magnetic Resonance Tomography

Within the last years, MRI has been increasingly applied for the analysis of bone structure and bone density. In order to determine bone density, quantification methods of susceptibility artefacts between bone marrow and trabecular bone marrow are applied. In bone marrow, this leads to a phase unwrapping of transverse magnetization with a shortening of relaxation time $T2^*$; the calculated parameter demonstrates a good correlation with bone density.

High-resolution MRI is used for analysis of bone structure, making it possible to achieve a spatial resolution in vivo of about 150 μm and slice thickness of 0.5 mm. Gradient echo (GRE) and spin echo (SE) sequences are mainly applied. Al-

though GE sequence is more susceptible to artefacts, its examination time of about 7 minutes is noticeably shorter than in SE sequences with better signal-to-noise ratio. For best possible depiction of the trabecula, the shortest TE possible ($TW < 10$) is recommended.

Disadvantages of MRI up until now include its applicability to only peripheral extremities and the relatively high number of artefact-specific influences. Therefore, the highest-achievable standardisation of acquisition techniques is required.

The most established parameter for structural analysis using a high-resolution imaging method is based on histomorphometric criteria, for example the number of trabeculae, trabecular thickness, and trabecular separation.

38.3.2 Types of Osteoporosis

- **Generalised Osteoporosis**
- ■ **Postmenopausal Osteoporosis**

Postmenopausal osteoporosis, classified as **Type I osteoporosis**, is the most common form of osteoporosis. Women between the ages of 50–65 show an increased resorption of cancellous bone. Because of higher bone turnover, these changes are revealed earlier than changes in cortical bone. Factors that play a role in postmenopausal osteoporosis include hormones, physical activity, and diet. Clinical signs of osteoporosis are ostealgia, loss of height, and increased kyphosis caused by vertebral fractures. Spinal deformities and fractures of the distal radius are common, whereas proximal femoral and rib fractures are less common.

- ■ **Senile Osteoporosis**

Type II osteoporosis is also known as senile osteoporosis. It is characterised by proportionate bone density loss in cancellous and cortical bone. Senile osteoporosis differs from postmenopausal osteoporosis in the sense that fractures of the femoral neck, subcapital humerus, spine, distal radius, pelvis, and tibia are common in both women and men above the age of 75 years. The aetiology is multifactorial, including age-associated loss of physiologic new bone formation, reduced kidney function, calcium deficiency, and age-associated secondary hyperparathyroidism.

- ■ **Secondary Osteoporosis**

Cushing Syndrome and Corticosteroid Osteoporosis Cushing syndrome is characterised by an excessive level of either endogenous or exogenous glucocorticoids. This leads to a decrease of osteoblastic activity and simultaneous increase of new bone formation.

The main cause of **endogenous** Cushing syndrome is adrenocortical hyperplasia; less common causes include tumours of the adrenal glands, hypophysis, or paraneoplastic diseases. It most commonly affects women between the second and sixth decade of life.

Corticosteroid osteoporosis occurs in patients having undergone transplant, patients with rheumatic diseases, autoimmune diseases, and all other diseases associated with long-term corticosteroid medication of high dosage. Older and postmeno-

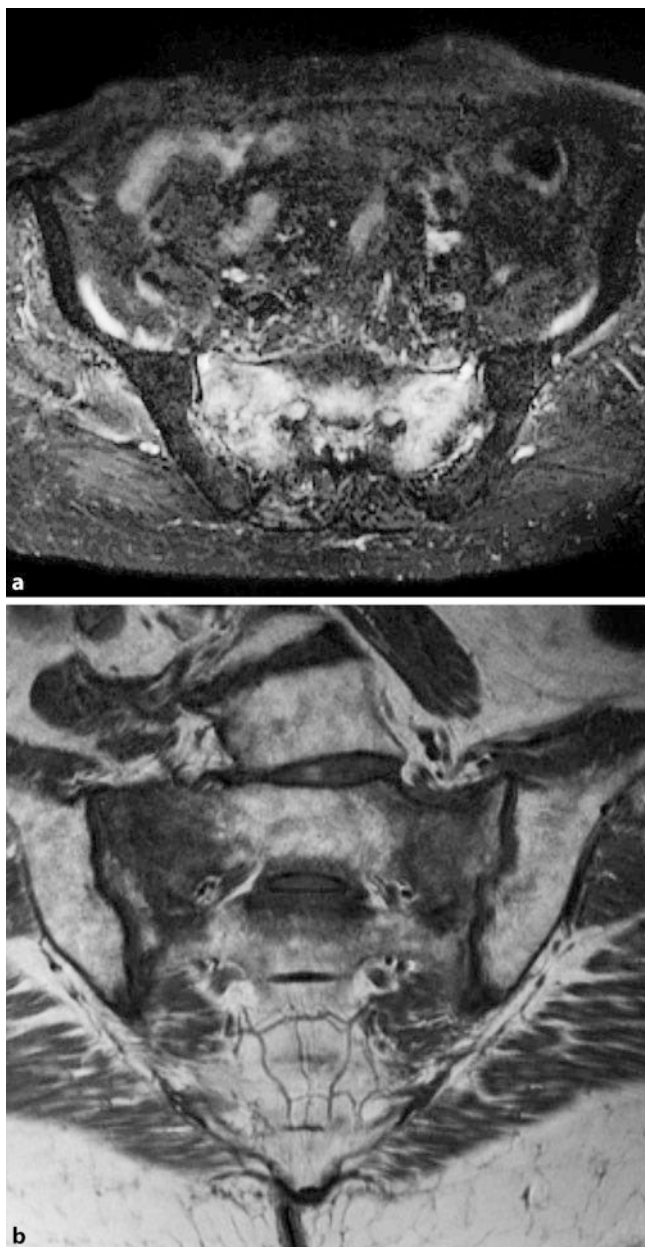


Fig. 38.13a,b MRI of the sacrum in a postmenopausal patient after cortisone therapy. **a** On the STIR sequence, evidence of a regional oedema with bilateral fatigue fracture of the sacrum. **b** On the coronal T1-weighted image the fracture lines are shown as hypointensity

pausal women tend to present this type of osteoporosis with clinical symptoms of obesity, “moon face,” muscle weakness, emotional instability, abnormal hair growth, ostealgia, and hypertension.

Imaging. Osteoporosis demonstrates radiolucency in the spine, pelvis, ribs, and skull. Vertebral changes are characterised by rarefaction of the architecture of cancellous bone, emphasised base-and endplates, and in later stages spinal deformity. Although this type of osteoporosis is not differentiable in imaging from postmenopausal and senile osteoporosis, there is usually **pronounced callus formation** in the vertebrae and ribs. **Pelvic stress fractures**

are common for this type of osteoporosis. These fractures are diagnosable at the moment only in MRI and in supplementary CT (■ Fig. 38.13).

Osteonecrosis is another indication of osteoporosis occurring more frequently in the exogenous form than the endogenous form. The most common site is the proximal femur, but changes may also occur in the proximal humerus and diffuse in bone marrow of long bones as well.

Osteoporosis in Haematologic Systemic Diseases In some haematologic systemic diseases, medullary space infiltration causes diffuse demineralisation. In addition to plasmacytoma, this group of disorders includes metastatic diseases, lymphoma, leukaemia and thalassaemia, sickle cell anaemia, and Gaucher’s disease. Plasmacytoma in particular demonstrates diffuse osteopaenia in the area of the truncal skeleton which is undifferentiable from osteoporosis in conventional imaging. In the event of suspicion, supplementary MRI is useful for differentiation.

Additional Types of Osteoporosis Syndromes such as **hyperparathyroidism**, **hyperthyroidism**, and **acromegaly** can cause osteoporotic changes. **Exogenous causes** for osteoporosis are high doses of the medication heparin, immunosuppression, and alcohol abuse.

A rare form of this disease is **juvenile osteoporosis**, which mostly presents with spinal deformity and consecutive kyphosis prior to puberty. Metaphyseal fractures of peripheral bone are common in the knee and ankle. Differential diagnosis of juvenile osteoporosis considers osteogenesis imperfecta, in which changes of bone quality are most significant.

- **Localised Forms of Osteoporosis**
- ■ **Osteoporosis Caused by Inactivity**

Osteoporosis caused by inactivity mainly arises in immobile bone areas following trauma or paralysis. In younger patients these changes are evident at an earlier stage, for example two to three months earlier, due to active bone metabolism. The peripheral extremities are by far the most affected areas, most commonly accentuated by homogenous demineralisation and less commonly by a pattern resembling a finely dotted ribbon, in this case metaphyseal and subchondral.

Differential diagnosis of osteoporosis caused by inactivity must consider Sudeck’s disease. Sudeck’s disease, a reflex bone dystrophy, also presents swelling, hyperesthesia, vasomotoric changes, and limited motion of an extremity caused by post-traumatic neural reaction. Conventional X-ray in Sudeck’s disease demonstrates a soft tissue swelling in combination with a type of osteoporosis that can be very aggressive. Ribbon-forming or dotted areas of demineralisation in the metaphysis are present. In addition, there are subperiosteal and intracortical resorption zones as well as erosive subchondral, juxta-articular changes in the sustained area between the joints. Unlike osteoporosis caused by inactivity, radiologic changes are noticeably much more pronounced; nevertheless, clinical symptoms play a greater role in differentiation (between Sudeck’s disease and Osteoporosis caused by inactivity) (■ Fig. 38.14).

■ **Fig. 38.14a,b** Osteoporosis caused by inactivity. **a** Following surgery of radius fracture, demineralization of wrist bones with no evidence of trophic changes. **b** In the later course of the disease remineralisation can be seen



■ ■ Transient Osteoporosis

Transient osteoporosis occurs predominately at the hip. It is of unclear aetiology, occurring most frequently in men between the third and fourth decades and in pregnant women during the third trimester. Patients present with non-traumatic pain that generally begins to decrease within two to six months.

Imaging. Several weeks following the start of the disease, conventional X-ray demonstrates demineralisation of the femoral head and less commonly of the femoral neck and acetabulum. Already in the early stages of the disease, MRI reveals bone marrow oedema in the proximal femur (■ Fig. 38.15).

Another form of osteoporosis that tends to develop in the knee, ankle, and foot is **regional, migratory osteoporosis**. This form most frequently occurs in men between the ages of thirty and fifty. Clinical symptoms include pain and swelling in the affected region of the body over a period of up to nine months.

38.3.3 Osteomalacia

■ ■ Definition

Osteomalacia is a secondary ossification disturbance leading to absent or decreased mineralisation of the organic bone matrix with consecutive accumulation of the mechanically less resistant osteoid.

■ ■ Pathophysiology, Aetiology

Osteomalacia serves as an umbrella term for diseases with a pathophysiological aetiology in active vitamin D deficiency, vitamin D metabolic disease, primary calcium deficiency, and

disrupted phosphate metabolism. Vitamin D causes an increasing absorption of calcium in the gastrointestinal tract. In bone it leads in low concentrations to an increased mineralisation of the bone matrix but in higher concentrations to an increased mobilisation of calcium and phosphate.

Vitamin D also has direct influence on the tubular calcium reabsorption of the distal renal tubule as well as a suppressing effect on parathormone secretions of the parathyroid glands. The synthesis of activated vitamin D depends determinately on the metabolic procedure of the liver and kidneys.

The following causes of osteomalacia are known:

- Vitamin D deficiency with calcium resorption disorder
- Dietary calcium deficiency
- Elevated enteral loss of calcium
- Phosphate deficiency
- Aluminium poisoning
- Tubular kidney damage
- Long term anticonvulsant therapy

➤ **Unlike osteomalacia, which develops in mature trabecular bone, rickets predominantly develops in the epiphyseal plates. Pathomechanisms of both diseases are identical.**

Osteomalacia leads to an excessive formation of osteoid that expands around trabecular bone and along the Haversian canals. Rarefaction of trabecular bone increases in number and diameter in simultaneously expanding and irregular Haversian canals.



■ Fig. 38.15a–c Transient osteoporosis of the proximal femur. a Radiograph reveals mildly pronounced demineralisation. b Corresponding image in fat-suppressed intermediate-weighted TSE sequence. c Subsequent signal decrease in the T1w sequence

■ ■ Imaging: Findings

Osteomalacia demonstrates unspecific demineralisation with reduction of trabecular bone structure that appears coarsened and blurry. It leads to intracortical bone resorption in long bones, pseudofractures, and Looser's zones. These appear in conventional X-ray images as line-forming transverse lucencies that usually only partially involve the diameter of the bone. Common locations of manifestation are the ribs, medial proximal

femur, scapula, pubic bone, and proximal ulna. These zones are mostly symmetric and surrounded by a sclerotic area, and they sometimes show periosteal callus formations. In the long-term course of the disease, long bone deflection can occur, in which case Looser's zones are usually located in the crest of the curve (■ Fig. 38.16).

A special form of osteomalacia (rickets in adolescents) causes changes in regions of the body with active bone growth.



■ **Fig. 38.16a,b Osteomalacia.** **a** Coarse thinning and striation of phalangeal compacta in a patient with osteomalacia. **b** Looser zones in CT in area of right rib 6 and 7 within context of a pseudofracture with surrounding symmetric sclerosis and periosteal callus-like bone apposition

An early sign is the widening of epiphyseal plates whose margins become increasingly blurred. The metaphyseal ends are spread apart and the diaphysis demonstrates a washed-out structure of cancellous and intracortical bone resorption. Distension of the costochondral junction, known as **rickets rosary**, is a common feature. Additional radiologic features are the outward curve of long bones, scoliosis, dislocated femoral head epiphyses, triangular pelvis, and impressions at the base of the skull. On the whole, patients generally show growth retardation.

➤ **Washed-out appearance of the spongiosa, thinning of compact bone, and Looser's zones are common signs of osteomalacia.**

38.3.4 Hyperparathyroidism

■ ■ Definition and Pathophysiology

The parathyroid hormone is one of the most important substances for regulation of bone and calcium metabolism. It elevates blood calcium levels and stimulates bone tumour with its influence on osteoclasts and milder influence on osteoblasts. The result is a subperiosteal, subchondral, and intracortical bone resorption found in early stages of the disease, especially in the hand.

Classification of hyperparathyroidism

There are three types:

- **Primary hyperparathyroidism** develops due to autonomy of the parathyroid gland. Solitary adenomas (50–80%) and diffuse hyperplasia (10–40%) of parathyroid glands are its most common causes. Multiple adenomas (ca. 10%) and parathyroid carcinoma (1–4%) are less common causes on a notable scale. Elevated serum calcium is a common finding in laboratory studies. Multiple endocrine neoplasm (MEN type I/IIA) is the most important consideration in differential diagnosis of primary hyperparathyroidism.
- **Secondary hyperparathyroidism** is the result of chronic hypocalcaemia. Its main causes are chronic renal failure or intestinal malabsorption with consecutive hyperplasia of parathyroidal bodies. In chronic renal failure, the calcium serum level is low to normal while phosphate values are high. Because of its association with changes of soft tissue and bone, this disease is also known as renal osteodystrophy.
- **Tertiary hyperparathyroidism** is the result of secondary hyperparathyroidism. The parathyroid develops autonomy with concomitant hypercalcemia.

In hyperparathyroidism, **three types** are distinguished (see above). **Pseudohyperparathyroidism** describes hypercalcemia occurring with suppressed parathyroid hormone secretion in pre-existing malignant neoplasia.

■ ■ Imaging: Radiologic Findings

A pathognomic change of hyperparathyroidism is the **subperiosteal resorption** of mineralised, cortical bone matrix. A typical site of occurrence is in the phalanges of the hand, especially on the radial side in the area of the middle phalanges II and III (■ Fig. 38.17). Additional predilection sites are the terminal tufts, long bones, ribs, and skull. Changes occurring near the joint resembling destruction caused by rheumatoid arthritis can also appear in hands and feet.

Unspecific findings are intracortical bone resorptions, which occur in other diseases with elevated bone turnover as well. The cortex of metacarpal II is a common location.

Subchondral resorption of mineralised bone matrix is present in the acromioclavicular joint, sacroiliac joint, and the symphysis. Resorptions can also occur in the spine and extremity



■ **Fig. 38.17a,b Hyperparathyroidism.** **a** Typical subperiosteal resorption in a patient with hyperparathyroidism emphasised radially at the second and third middle phalanx. **b** Same finding at the terminal tufts

joints. Subchondral bone can crack depending on severity and spinal intraspongious disc herniation can form. In cases of resorption at the sacroiliac joint, differential diagnosis must consider sacroiliac arthritis of Bechterew's disease.

In the skull there is a "salt and pepper pattern" caused by **trabecular bone resorption** as well as resorption changes in the dental alveolar chamber.

These changes, like brown tumours, are generally a sign of advanced disease. **Brown tumours** are common in primary hyperparathyroidism but can also occur in secondary hyperparathyroidism. Brown tumours consist of fibrous material, giant cells, cysts, and necrosis. Predilection sites are the pelvis, ribs, femur, and facial skeleton.

Along with the lytic and resorption findings mentioned above, **multiple areas of sclerosis** develop especially in secondary hyperparathyroidism in vertebral base- and endplates, the skull, and in the metaphysis in long bones. Calcium pyrophosphate deposits (**chondrocalcinosis**) also occur in the joints; these are especially indicative of primary hyperparathyroidism but may also, though less frequently, be a sign of secondary hyperparathyroidism.

Differential Diagnosis. Because of very characteristic subperiosteal resorption, radiologic diagnosis of hyperparathyroidism is generally unproblematic.

Intracortical bone resorption also occurs in other diseases with elevated bone turnover, for example hyperthyroidism and acromegaly. Cracks in the subchondral bone have a possible differential diagnosis of osteonecrosis, chondrocalcinosis, and arthritis.

Differential diagnosis in cases involving the hand bones includes rheumatoid and psoriatic arthritis; the main difference is the normal size of the joint space in hyperparathyroidism. Involvement of the sacroiliac joint should differentiate hyperparathyroidism from ankylosing spondylitis.

Brown tumours can imitate primary and secondary bone tumours; in such cases, diagnosis tends to be made within the whole context of the disease. In the differential diagnosis of sclerotic lesions Myelofibrosis, mastocytosis, metastasis, sarcoidosis, Paget's disease, and changes following radiation should be considered. In cases of soft tissue calcification, calcium pyrophosphate deposition disease (CPPD) should be taken into consideration.

38.3.5 Renal Osteopathy

■ ■ Definition

Renal osteopathy or dystrophy is a bone disease in patients with chronic renal failure. There are several characteristic components to this disease: first and foremost, secondary hyperparathyroidism and osteomalacia. Additional findings that occur are similar to osteoporosis and soft tissue and vascular calcifications.

■ ■ Imaging: X-Ray Findings

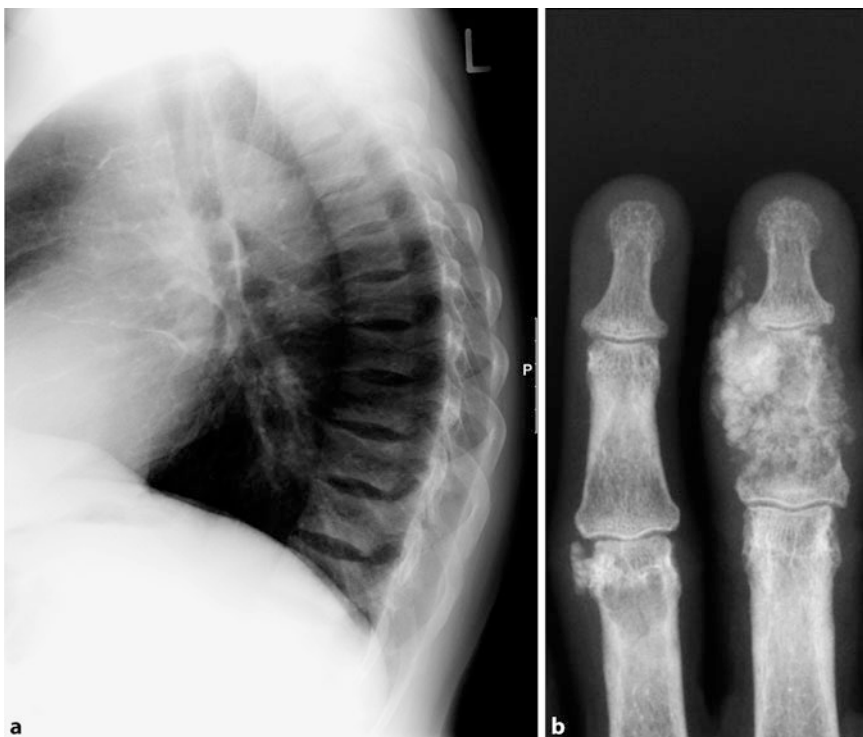
Comparable to secondary hyperparathyroidism are:

- subperiosteal bone resorption, pronounced in phalanges
- generalised cortical thinning
- decrease in bone density

Subchondral bone resorption, osteosclerotic changes, and brown tumours are also observed. A characteristic finding is wide, ribbon-like sclerotic changes of vertebral base- and endplates known "Rugger Jersey Spine" (■ Fig. 38.18). Additional areas of multiplied osteosclerosis are the pelvis, ribs, and the peripheral extremities. The long bones are mostly metaphyseal affected, less so also epiphyseal.

Chondrocalcinosis occurs noticeably less in renal osteopathy in comparison to primary hyperparathyroidism. Periosteal ap-

Fig. 38.18a,b Renal osteopathy. **a** Lateral X-ray image of thoracic spine with renal osteopathy. Sclerotic zones of vertebral body endplate and increased opacity of “rugger-jersey spine.” **b** Expanded periarticular calcification at the middle phalanx D3 representing pseudotumoural calcinosis



positions occur in 10–25% of patients, mostly in the metatarsals, femur, and pelvis and less so in the humerus, radius, ulna, tibia, metacarpals, and phalanges.

Furthermore, imaging characteristics of osteomalacia are evident in renal osteopathy but are somewhat difficult to differentiate from diseases with similar imaging features. Osteopaenia and Looser's zones are changes associated with osteomalacia; they occur comparatively less in renal osteodystrophy. In advanced stages of the disease, bowing of the long bones, malformation of the pelvis, and stress fractures can occur.

Soft tissue- and vascular calcification is relatively common in renal osteopathy. Calcification occurs in all tissue, for example in the corneal, visceral, subcutaneous, and periarticular tissue. Periarticular calcifications tend to have a very pronounced appearance and a tumour-like character; they are characterised as (pseudo)tumourous calcinosis. Predilection sites of partially bilateral occurrences include the hip, knee, shoulder, and wrist (■ Fig. 38.18).

Differential Diagnosis. Rheumatic diseases that cause erosive changes, for example rheumatoid arthritis and seronegative spondyloarthritis, must be differentiated from renal osteodystrophy. In addition, infectious and neoplastic processes can cause comparative changes; brown tumours and amyloid deposits can resemble primary and secondary bone tumours. Medical history and clinical presentation play a determining role in diagnosis.

■ ■ Associated Diseases

Patients with chronic renal insufficiency can also develop hyperuricaemia with resulting gout. In addition, oxalosis and a second-

ary amyloidosis can arise as a very rare complication of renal insufficiency. These bone changes can regress again following hemodialysis. On the contrary, an increase of osteopaenia with spontaneous fractures can occur. An additional complication of dialysis is septicemia, which can lead to osteomyelitis and arthritis. Destructive, aseptic spondyloarthropathy can also arise that radiologically resembles infection, neurogenic osteoarthropathy, or CPPD can also occur. After kidney transplantation, because of the corticosteroid therapy and the administration of immunosuppressants, increasing osteoporosis, spontaneous fractures as well as an increased appearance of osteonecrosis are the result especially in the femur, humerus head and talus. Incidence of arthritis and osteomyelitis is also elevated.

38.3.6 Hypoparathyroidism

■ ■ Definition, Aetiology, Clinical Presentation

Hypoparathyroidism is characterised by a hypofunction of the parathyroid. Aetiology differentiates a primary (or congenital) form from the secondary form. Primary or idiopathic hypoparathyroidism exists in aplasia or a hypoplasia of the parathyroid. Secondary or inherited hypoparathyroidism mainly develops following thyroid surgery or as result of cervical radiation.

Patients with hypoparathyroidism show above all neuromuscular symptoms caused by low calcium levels.

■ ■ Imaging: X-Ray Findings

Diffuse or localised osteosclerotic changes are the most common imaging feature. A thickening of the skull is typical, whereas thickening in the facial skull is less common. Compli-

cations include intracranial elevation of pressure and development disorders of teeth. In addition, intracranial calcification occurs in the area of the basal ganglia, cerebellum, and the choroid plexus. Osteosclerotic bands occur in the metaphysis of long bones, the ilium, and more mildly in the vertebral bodies.

Subcutaneous calcification is an additional imaging feature that predominantly occurs in the hip and shoulder joints. Changes occur less frequently in the area of the spine, are associated with calcification of ligaments, and as a maximal variant can lead to changes similar to those in diffuse idiopathic skeletal hyperostosis (DISH).

Differential Diagnosis. Diffuse or localised osteosclerosis is present in renal osteopathy, myelofibrosis, mastocytosis, Paget's disease, and osteoblastic metastases. Skull thickening is, however, a relatively typical characteristic of hypoparathyroidism. The band-like thickening described above is also observed in hypothyroidism, hypervitaminosis, leukaemia treated by chemotherapy, and metallic poisoning.

Basal ganglia calcification is common in hypoparathyroidism and pseudohypoparathyroidism, but can also occur in Fahr's syndrome, toxoplasmosis, cytomegalovirus, and cases of poisoning. Subcutaneous calcification is an unspecific finding also evident in renal osteopathy, collagenosis, and a chronic vitamin D overdose.

38.3.7 Pseudohypoparathyroidism

■ ■ Definition, Epidemiology, Clinical Presentation

Classical pseudohypoparathyroidism is characterised by low serum calcium and an elevated phosphate levels. This condition is primarily associated with a normal parathyroid gland, but due to renal end-organ resistance parathormone values are nevertheless elevated. Albright was the first to describe classical pseudohypoparathyroidism as characterised by stunted growth, short neck, round face, and shortened metacarpals. This disorder also involves mental deficiency, strabismus, disruption of the olfactory gland, and dental problems. It occurs more frequently in women and is usually diagnosed in the second decade of life.

➤ **Pseudohypoparathyroidism has a rare identical phenotype with unnoticeable laboratory findings and absent end-organ resistance.**

■ ■ Imaging: X-Ray Findings

Shortened metacarpals (especially the first, fourth, and fifth) and metatarsals caused by early closing of the epiphyseal plate are a common finding. Shortening and widening of the phalanges is present. In addition, soft tissue calcification and exostosis are evident.

38.3.8 Osteopathies in Hypo-/Hypervitaminosis

Osteomalacia is the most significant type of hypovitaminosis that affects the muscular skeleton. Hypovitaminosis A and C also exist as well as hypervitaminosis A and D.

■ Hypervitaminosis A

Chronic hypervitaminosis A is generally found exclusively in children presenting with clinical symptoms of itchy rash and anorexia. After weeks or months the formation of small nodules in the extremities can take place. Hepatosplenomegaly, clubbed fingers, and hair loss are also evident.

X-ray images of children in the first decade of life demonstrate cortical thickening with periosteal new bone formation. Common locations are the diaphysis of ulna and the metatarsals, whereas less common locations include the clavicle, tibia, and fibula. Cupping is demonstrated in the metaphysis, and a narrowing and premature closing of epiphyseal plates with consecutive growth disturbances and deformations is observed. Unlike the disruption of growth, excessive deposition of periosteal bone becomes reversible following decreased vitamin A intake.

■ Hypovitaminosis A

The primary effect of chronic vitamin A deficiency is on epithelial structures. It causes stunted growth, anaemia, and an elevated risk of infection in children. Musculoskeletal changes are rarely evident in radiologic examination.

■ Hypovitaminosis C (Scurvy)

Scurvy is very rare in western countries. It is a disease that mostly develops in children raised on a diet absent of fruits and vegetables.

Infantile scurvy develops between 4–10 months following vitamin C intake. Clinical presentations include haemorrhage and soft tissue inflammation. It leads to decreased cellular activity in the metaphysis and epiphysis. Detritus and infarction develop in the epiphyseal plates.

Imaging examination demonstrates a widening of the growth plates; an increased sclerotic band of radiolucency in the metaphysis known as the Trümmerfeld zone is evident. Small metaphyseal spurs are also present and demineralisation with atrophy of the spongiosa occurs in the diaphysis. In addition, subperiosteal haematoma with calcification can be present. Conversely, stunted growth is rare.

Adult scurvy is very rare and is only present in cases of extreme malnutrition. Within a context of haemorrhagic diathesis, joint bleeding is present. Central and peripheral osteoporosis with vertebral deformation is also evident.

■ Hypervitaminosis D

Chronic vitamin D toxicity presents clinical symptoms of polyuria, polydipsia, vomiting, anorexia, diarrhoea and stomach pain. Laboratory examination includes hypercalcaemia, hypercalciuria, haematuria, and albuminuria.

In children, a thickened metaphysis represents calcified growth zones. Cortical bone demonstrates partial thickening that not only leads to osteosclerosis but also osteopaenia. Calcification

of vessels, visceral organs, muscles, and periarticular calcification is also evident.

In adults, a vitamin D overdose can appear as peripheral or central osteoporosis. Extended periarticular soft tissue calcification is observed in bursae, ligaments, sinew, joint capsules, and in the joint space. Differential diagnosis must consider hyperparathyroidism, renal osteopathy, plasmacytoma, and bone metastasis. Furthermore, soft tissue calcification is evident in collagenases, necrotic changes, and in milk-alkali syndrome.

38.3.9 Endocrine Bone Diseases

The most significant endocrine diseases are osteoporosis, hyperparathyroidism, and acromegaly. The following paragraphs outline the effects of thyroid malfunction and diabetes on the musculoskeletal system.

■ **Hyperthyroidism**

Thyroid hyperfunction causes the overproduction of thyroxin and triiodothyronine. The suspect causes are autonomic adenoma or Basedow's syndrome, which is an autoimmune disease. Patients clinically present with nervousness, tremors, hyperhidrosis, weight loss, diarrhoea, tachycardia, and cardiac arrhythmia. Catabolic changes in bone occur which lead to elevated calcium and phosphate serum levels, an increase of alkaline phosphate, and hypercalciuria.

■ ■ **Imaging: X-Ray Findings**

Radiographic findings of hyperthyroidism usually become evident only after several years. In this case, men are more frequently affected than women. Primary sites for the development of osteoporosis are the axial skeleton, skull, and the hands and feet. Osteoporotic changes in the spine tend to demonstrate rarefaction of spongiosa structure and vertebral deformities, and osteoporotic sintering can cause multiplied thoracic kyphosis. Imaging characteristics resemble those observed in senile osteoporosis. Occurrences in the distal radius and femoral neck are elevated. In children, bones may mature too quickly. Myopathic changes are not visualised in imaging studies.

Thyroid Acropachy and Differential Diagnosis. **Thyroid acropachy** is a rare manifestation of hyperthyroidism that mostly occurs following therapy. Clinical symptoms include pretibial oedema, exophthalmos, clubbing of the fingers, and painless swelling of the distal extremities. Periosteal bone formations at the metacarpals and the proximal and middle phalange are evident in imaging studies. They demonstrate solidity, accentuated radial and irregular margination with a somewhat stringy appearance.

Diagnosis must differentiate thyroid acropachy from hypertrophic osteoarthropathy, the latter of which generally occurs in the tibia, fibula, and radius. An identical classification with additional typical skin changes of the face indicates pachydermoperiostosis. Hypervitaminosis A and venous stasis also demonstrate periosteal changes but display different characteristics in both imaging studies and clinical presentation than acropachy.

■ **Hypothyroidism**

An underactive thyroid in primary hypothyroidism leads to insufficient or deficient production of thyroxin and triiodothyronine. Secondary hypothyroidism is characterised by a decreased presence of thyroid-stimulating hormone (TSH). Aetiology includes thyroid atrophy, thyroiditis, tumour infiltration, certain medications, or a condition following surgery of the thyroid or radiation therapy. Clinical symptoms are lethargy, bradycardia, hypotonia, myxoedema, and obstipation. In children, an underactive thyroid leads to cretinism, mental retardation, developmental disruptions of bone, and pretibial myxoedema.

■ ■ **Imaging: X-Ray Findings**

Changes in paediatric cases are very pronounced in imaging. Brachycephaly, enlarged sella turcica, prognathism, and improper aeration of noval sinus may occur. Epiphyseal dysgenesis is evident in the area of the femoral and humerus head as well as the navicular bone.

Differential diagnosis considers Perthes disease and Kohler disease. Another complication in conjunction with thoracolumbar spine malformation is femoral head epiphysiolysis.

Conversely, changes in adults are extremely discrete: osteoporosis may occur and an elevated incidence of carpal tunnel syndrome is observed. Furthermore, joint and bone pain related to articular effusions, soft tissue swelling, and calcification can be present as well as muscle cramps and increased stiffness.

■ **Diabetes Mellitus**

Diabetes mellitus is the cause of many musculoskeletal diseases:

- Diabetic neuro-osteoarthropathy
- Septic osteomyelitis and arthritis
- Degenerative joint changes
- Diffuse idiopathic skeletal hyperostosis (DISH)
- CPPD disease
- Soft tissue changes such as Dupuytren's contracture, tenosynovitis, peri-arthritis, and carpal tunnel syndrome

Diabetes is the most common cause of **neuro-osteoarthropathy**. Diabetic neuropathy leads to a loss of pain sensibility especially in the lower extremities. Additional factors of the disease include decreased circulation in arteriosclerotic vascular wall changes.

In **imaging studies**, osteolysis, osteosclerosis, and severe joint destruction, especially of the intertarsal, tarsometatarsal, and metatarsophalangeal joints, are evident (■ Fig. 38.19). In later stages of the disease, spontaneous fractures, luxation, and infections are common. A special reversible form of diabetic osteoarthropathy involves nonreactive osteolysis in the distal metatarsals and proximal phalanges.

An additional but common complication is soft tissue ulceration and infection, in particular of the foot, which can spread secondarily to bones and joints. Common regions of spread are the first and fourth metatarsophalangeal joint and underneath the calcaneus.

Dupuytren's contractures with fibrotic changes that may spread to metacarpophalangeal and proximal interphalangeal joints are common in diabetic patients. Pain is also present in the



Fig. 38.19a,b Diabetic neuro-osteoarthropathy. a, b Charcot foot related to diabetic neuro-osteoarthropathy demonstrating bone destruction in the Chopart joint and sinking of the foot arch

rotator cuff, where soft tissue calcification in tendons or bursae can sometimes occur.

38.3.10 Bone Diseases caused by Toxicity

■ Heavy Metal Toxicity

■ Lead

Lead poisoning is mainly caused by ingestion of lead paints or inhalation of lead-based fumes, for example following the burning of batteries. Lead ammunition can also cause poisoning in the event that they for example come into contact with a joint. Cases of chronic poisoning demonstrate encephalopathy with pain, delirium, or coma, in some cases neuritis, stomach pain, and anaemia.

Imaging. In imaging examination, strong sclerotic lines are evident in the metaphysis of long bones, mostly in the knee joint. In

advanced stages of the disease, these lines are also noticeable in the fibula. After removal of chronic lead poisoning, sclerotic lines will disappear within several years. **Differential diagnosis** must distinguish these lines from physiologic growth lines and other lines caused by growth disturbances such as rickets, scurvy, hypothyroidism, hypoparathyroidism, and leukaemia. In children, additional signs of lead poisoning are stunted growth in long bones with metaphyseal distension.

■ Aluminium

Aluminium poisoning is related to dialysis or the ingestion of large amounts of aluminium-based antacids. Aluminium deposits in bones and the brain and can lead to dialysis encephalopathy.

Imaging. Radiologic examination demonstrates osteopaenia, changes resembling rickets with Looser's zones, periostitis, and pathologic fractures.

■ Bismuth

Bismuth toxicity occurs in association with the treatment of syphilis. Foetal bone deposits with sclerotic lines due to placenta transfer resemble the sclerotic lines seen in lead poisoning. Osteonecrosis can sometimes be evident in adults.

■ Drug-Induced Bone Diseases

■ Fluoride

Chronic fluoride poisoning is observed in industrial and laboratory workers and in patients with medications containing a high dose of fluoride. Ninety-nine percent of ingested fluoride is saved in the body in mineralised tissue. Patients suspicious of fluoride poisoning present with joint pain, lower back pain, paraplegia, dyspnea, and palpable hyperostosis.

Imaging. X-ray portrays sclerotic changes of the axial skeleton with decreased pronouncement in the long bones and skull. Advanced stages can show spinal stenosis due to the development of spondylophytes. Parallel to periosteal new bone formation, fibroostosis is observed at the iliac crest, ischium, and underneath the origin of the ribs. Calcification occurs in the paraspinous, sacrotuberous, and iliolumbar ligaments and in the bones of extremities. Bone demonstrates decreased stability, leading to an elevated incidence of vertebral fracture.

Next to osteoblastic bone metastases, **differential diagnosis** must consider myelofibrosis, mastocytosis, renal osteopathy, and Paget's disease. Considerations must also include diffuse idiopathic bone hyperostosis (DISH), pronounced spondylosis, and acromegaly. Periosteal proliferations are also observed in hypertrophic osteoarthropathy, pachydermoperiostosis, and thyroid acropachy.

■ Milk-Alkali Syndrome

Milk-alkali syndrome defines the occurrence of hypercalcaemia without simultaneous hypercalciuria or hyperphosphataemia. It usually occurs in patients with repeated ingestion of milk and calcium carbonate in the attempt to control their elevated levels of stomach acid.

Imaging. X-ray demonstrates pronounced periarticular soft tissue calcification, vascular calcification, calcification of the kidneys, ligament structures and cerebral falx. Bone abnormalities cannot be imaged. **Differential diagnosis** considers hyperparathyroidism, renal osteodystrophy, hypervitaminosis D, collagenosis, and idiopathic tumoural calcinosis.

■ ■ Additional Medications

Long-term **ingestion of prostaglandin** in newborns leads to periosteal new bone formation, especially in the ribs and long bones but much less so in the mandibula, scapula, and clavicle.

Dilantin, heparin, methotrexate, and alcohol can cause osteoporosis. Osteomalacia is observed in long-term ingestion of **phenobarbital and phenytoin**.

38.4 Osteonecrosis and Bone Infarction

S. Waldt, M. Eiber

Osteonecrosis is characterised by a more or less localised necrosis of trabecular and compact bone, which almost exclusively affects the epiphysis or apophysis of bone.

On the contrary, **bone infarction** presents a form of necrosis that affects the trabecular bone and the bone marrow, usually in the metaphysis or metadiaphysis of the long tubular bones.

38.4.1 Osteonecrosis in Adults

Multiple etiologic factors (trauma, medication, e.g., cortisone, radiation therapy, vascular and metabolic diseases, infections) can play a role in causing osteonecrosis in adults. In the pathogenesis of osteonecrosis, however, disruption of osseous macro- and microcirculation with central consecutive cellular necrosis is always present.

■ Osteonecrosis of the Femoral Head

■ ■ Definition, Aetiology, Epidemiology

Because of the different aetiology idiopathic femoral head necrosis is distinguished from post-traumatic femoral head necrosis. The cause of post-traumatic femoral head necrosis is injury to the arteries supplying the femoral head. Following intracapsular (medial) femoral neck fractures, hip dislocations, and slipped capital femoral epiphysis femoral head necrosis occurs in a significant proportion of cases. Idiopathic femoral head necrosis occurs most frequently between the fourth and seventh decade of life. It affects men more often than women.

■ ■ Classification, Clinical Presentation, Imaging

Different classification guidelines were developed for defining the stages of femoral head osteonecrosis (■ Table 38.4, ■ Fig. 38.20). **Ficat and Arlet** is one of the oldest and still one of the most widely used classification systems; it takes into account clinical and radiographic findings. While symptomatic stage I demonstrates normal radiographic findings of the hip, stage II is char-

acterised by osteolytic and sclerotic changes within the necrotic segment. Stage III demonstrates flattening of the femoral head or evidence of a subchondral fracture (“crescent sign”). Stage IV reveals secondary osteoarthritic changes.

In clinical suspicion of femoral head necrosis in negative radiographic findings, MRI has been established due to its high sensitivity and specifically as the imaging modality of choice. In the early stage, the epiphyseal necrotic zone can be visualised on MR images usually as a sector-like segment with subchondral extension, generally hypointense on T1w with variable signal intensity on T2w images. In the literature evidence of subchondral signal changes (band lesions) above a certain size (length > 12 mm and width > 4 mm) on T2w or contrast-enhanced T1 images have been described as a finding with a very high predictive value for osteonecrosis.

The definite diagnosis of an osteonecrosis can be established in the further course of the disease by the evidence of a demarcation zone between the necrotic segment and the normal bone represented by the so-called “double line sign” on MR images. The “double line sign” can be seen on T2w or contrast-enhanced T1w images and is characterised by a high-signal-intensity inner zone (adjacent to the necrotic segment) and a low-signal-intensity outer zone (adjacent to the normal bone) consisting of an inner zone of granulation tissue and an outer zone of reactive bone sclerosis. In other localisations in the skeletal system this MRI sign, which is pathognomonic for osteonecroses, applies as well.

The **ARCO Classification** of osteonecrosis continues to become more established within German-speaking and other European countries (ARCO: Association internationale de la Recherche sur la Circulation Osseuse) (■ Fig. 38.20). Whereas the Ficat and Arlet classification system takes clinical findings into consideration, ARCO relies on imaging results (conventional radiograph, CT, MRI, and scintigraphy). Size and location of necrosis that are important factors for the prognosis of the disease are considered as subcategories in this classification.

■ **Table 38.4** Ficat and Arlet classification of osteonecrosis of the femoral head

Stage	Radiographic findings	Clinical presentation
0	Normal	Asymptomatic
1	Normal	Symptomatic
2	<ul style="list-style-type: none"> – Sclerotic areas (linear, diffuse, or localized) in the femoral head – Osteolytic or “cystoid” changes (usually more difficult to define) – Femoral head has normal shape and margins (!); no joint space narrowing 	Symptomatic
3	<ul style="list-style-type: none"> – Collapse and flattening of the femoral head with complete loss of bone structure – Large cyst-like lucencies, diffuse sclerotic changes 	Symptomatic
4	Secondary osteoarthritic changes	Symptomatic

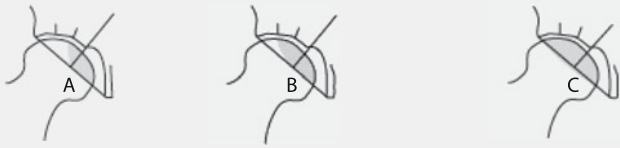
		ARCO stages				
		Stage 0	Stage 1	Stage 2	Stage 3	Stage 4
Imaging	X-ray	Normal	Normal	Sclerosis and osteolysis in the necrotic segment; sclerotic rim	Evidence of fracture; flattening of the femoral head	Additional arthrotic changes
	MRI	Normal	Area of necrosis	Necrosis with reactive rim; double-line sign	Evidence of fracture	Additional arthrotic changes
	CT	Normal	Normal	Sclerosis and osteolysis in the necrotic segment; sclerotic rim; asterisk sign	Evidence of fracture; inflammation of the femoral head	Additional arthrotic changes
	Scintigraphy	Normal	Diffuse or cold spot	Cold in spot	Hot in hot	Hot in hot
Subclassifications	Localisation of the necrosis	None				None
	Extent of necrosis	None	Proportion of the femoral head: A < 15% B 15–30% C > 30%		Extent of the subchondral fracture: A < 15%; B 15–30% C > 30% Flattening of the femoral head: A < 2 mm; B 2–4 mm; C > 4 mm	None

Fig. 38.20 Association internationale de la Recherche sur la Circulation Osseuse (ARCO) stages

ARCO Classification of Femoral Head Necrosis

- In **ARCO Stage 0** all imaging findings are negative. This is only a theoretical stage. As observed in animal studies, very early stages of ischaemia are missed on imaging studies.
- In **ARCO Stage 1** (reversible early stage) radiographs and CT show no pathologic findings. On MRI, signal alterations are evident in a bone segment with subchondral extension without evidence of a demarcation zone. Scintigraphy may demonstrate diffuse increased activity consistent with reactive hyperaemia or “cold spots” due to reduced blood flow in the necrotic zone. Furthermore, ARCO classification determines a medial (A), central (B), and lateral (C) location and the extent of necrosis [$< 15\%$ (A), $15\text{--}30\%$ (B), $> 30\%$ (C)]. Prognosis in sub-stage C is generally poor.
- **ARCO Stage 2** (irreversible early stage) is characterised by delineation of the necrotic segments via a demarcation zone. Radiographs and CT demonstrate a sclerotic rim bordering the necrotic segments. On MR images “the double line sign” consisting of a high-signal-intensity inner zone (adjacent to the necrotic segment) and a low-signal-intensity outer zone (adjacent to the normal bone on T2w images or contrast-enhanced images delineates the necrotic segment (see above). At scintigraphy the corresponding

finding is the “cold in hot spot” sign that is pathognomonic with enhancement of rim zone and missing activity in the necrotic zone. Subclassification is as in stage 1.

- **ARCO Stage 3** is defined by fracture. This can appear as a subchondral fracture, “crescent sign,” or as a collapse or flattening of the femoral head. The detection of a subchondral fracture as a linear, crescent-shaped radiolucent line on radiographs and CT is called a “crescent sign.” Correspondingly, a high-signal band-shaped zone can be visualised on T2-weighted MR images representing joint fluid entering the fracture zone. Scintigraphy shows in Stadium 3 a “hot in hot spot.”
- In ARCO stage 3 subclassification results from the extent of the subchondral fracture line ($< 15\%$ A, $15\text{--}30\%$ B, $> 30\%$ C) and amount of flattening of the femoral head [< 2 mm (A), $2\text{--}4$ mm (B), > 4 mm (C)]. Location is correspondingly determined with subclassification of stages 1 and 2.
- **ARCO Stage 4** is defined by the development of secondary osteoarthritis. The classic signs of osteoarthritis with joint space narrowing, subchondral sclerosis, cyst formation, and osteophytes are evident on radiographs, CT, and MRI. Scintigraphy exhibits increased activity in the sense of a “hot spot.”

Although the ARCO classification system is applicable to all imaging modalities, MRI is still considered the modality of choice for determining and diagnosing early stages of femoral head necrosis. MRI best defines the exact extent and precise location of necrotic segments. In later stages CT is considered the modality of choice for the detection and determining the extent of fracture.

■ ■ Therapy

The prognostically and therapeutically most important criterion in assessment of femoral head necrosis is evidence of fracture. As flattening of the femoral head is a significant predisposing factor of osteoarthritis, a long-term femoral head conserving therapy is only possible in rare cases.

■ Ahlbäck's Disease

■ ■ Localisation, Epidemiology, Clinical Presentation

The idiopathic (spontaneous), mostly unilateral osteonecrosis at the knee joint usually manifests in the loading zone of the medial femoral condyle. Rarely, the lateral condyle, the medial or lateral tibial plateau are affected. Ahlbäck's disease mostly affects older, often female patients. Sudden pain in the area of the medial femoral condyle is characteristic.

■ ■ Imaging

Immediately after the appearance of symptoms **conventional radiographs** are usually unremarkable. After a few weeks, as well as the discrete thickening of the subchondral cancellous bone, flattening of the femoral condyle is visible. After 2–3 months subchondral radiolucent zones are found; demarcation of the area of necrosis by a surrounding sclerosis is discernible. In the later course cracking of the cortex or sintering of the femoral condyle occur.

Using MRI the diagnosis of Ahlbäck's disease can be made early and with great sensitivity. In the affected femoral condyle a circumscribed bone marrow oedema is usually evident. This can be very well delineated on fat-suppressed T2-, intermediate-, proton-density-weighted and on STIR images. As an early sign of osteonecrosis and a differentiation criterium with regard to transient bone marrow oedema, the evidence of subchondral band forming signal decreases is valid. The longitudinal extent of a hypointense area >14 mm, a thickness of >0.4 cm as well as a localisation in the depths of the condyle were described as being relatively certain indications for irreversible osteonecrosis. The distinct definition of the area of necrosis can be relieved by the application of intravenous contrast medium. The necrotic fragment is distinguished from the adjacent bone marrow oedema because of the lack of contrast medium uptake. MRI also enables evaluation of the cartilage coating of the affected femoral epiphysis.

■ Lunate Osteonecrosis

■ ■ Definition, Aetiology, Epidemiology

Synonyms: Kienbock's disease, osteomalacia of the lunate.

Necrosis of the lunate bone occurs frequently following one-time trauma but primarily following repetitive trauma of the

wrist in patients between the ages of twenty and forty. Men are more affected than women. Ulnar length deficiency is present in over 70% of all patients.

■ ■ Classification, Imaging

The Lichtman and Ross system is the most established classification of lunate osteonecrosis based on conventional radiographs in two planes. However, additional information provided by MRI and CT should be considered in this classification as well:

- Stage 1: bone marrow oedema within the lunate; only MRI is diagnostic, the lunate reveals a normal trabecular pattern and a normal shape; the other carpal bones are normal.
- Stage 2: changes of the bone structure with diffuse bone sclerosis and cystic inclusions, possible early fracture line on the radial site of the lunate; the shape of the bone is mandatory unchanged. The other carpal bones are normal.



■ Fig. 38.21 Osteomalacia of the lunate. DP radiograph of the wrist demonstrates progressive collapse of the lunate in stage 3 of osteonecrosis

- Stage 3A: fracture line on the proximal circumference; the lunate is slightly deformed, incipient collapse; normal carpal alignment.
- Stage 3B: fractured; the lunate is increasingly deformed; progressive collapse with fixed scaphoid rotation; increased density of the lunate (■ Fig. 38.21).
- Stage 4: the lunate is extremely dense; severe lunate collapse; osteoarthritis.

38.4.2 Osteonecrosis in Children and Adolescents

Synonym: Osteochondrosis.

Osteochondroses in adolescents mostly occur in a typical age timeframe and nearly all osteochondroses show a predilection for either boys or girls. ■ Table 38.5 and ■ Fig. 38.22 outline common sites of osteonecrosis, the name of the physician responsible for its first description, and the age of manifestation in which the osteochondrosis typically occurs.

Osteochondrosis defines a **heterogeneous group of diseases** that demonstrate characteristic imaging features of sclerosis, fragmentation, deformation, and often re-ossification and re-formation of the osseous contour of apophyseal or epiphyseal ossification centres. Next to primary (idiopathic) and secondary osteonecrosis, other disorders such as Sever's disease (thickening of the calcaneus apophysis) or Van Neck's disease (distension and irregularity of ischiopubic synchondrosis) are no longer considered as the result of aseptic osteonecrosis, but instead as variation in normal ossification. In other types of manifestation,

for example Scheuermann's disease, with an aetiology that traces back to trauma or abnormal stress, histology similarly does not demonstrate evidence of osteonecrosis.

The following paragraphs describe Perthes' disease, Scheuermann's disease, and osteochondrosis dissecans, which all belong to the group of osteochondroses.

■ Perthes Disease

■ ■ Definition, Epidemiology

Synonym: Legg-Calvé-Perthes Disease.

Perthes disease refers to aseptic (idiopathic) femoral head necrosis in children; incomplete ossification of the epiphysis with potential for healing defines its main difference to the adult form. The disease predominantly affects children aged four to eight; boys are affected at a ratio of 5:1 more frequently than girls. In ca. 10% of cases a bilateral manifestation takes place. In this case, a metachronic infliction of the femoral head is common. A synchronic occurrence in both femoral heads speaks against Perthes' disease and instead for a disease of different origin in the epiphysis.

In hypothyroidism and epiphyseal dysplasia, there is a similar, even sometimes identical radiographic morphology as in the fragmentation stage of Perthes' disease.

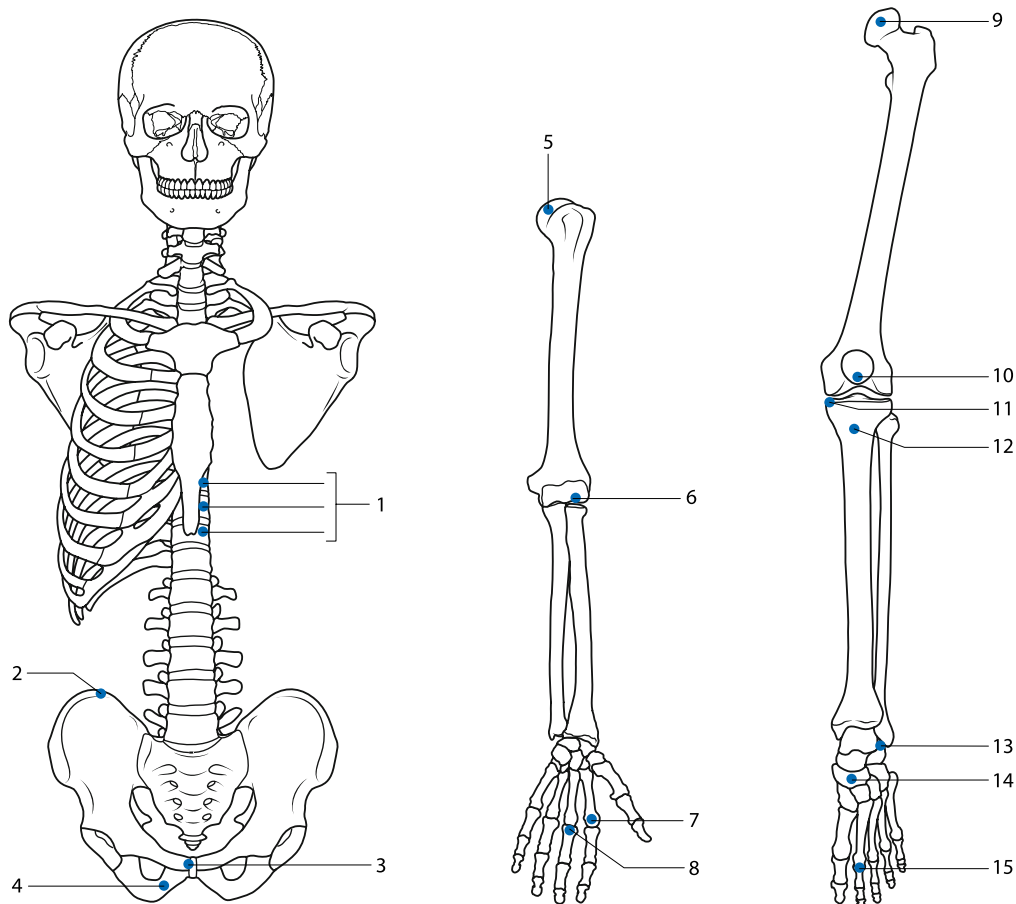
■ ■ Clinical Presentation

Resistance to hip abduction (adduction contracture) of the affected leg is common.

■ Table 38.5 Overview of location and age of manifestation of juvenile osteochondrosis

Location	Named by ...	Age of manifestation
1 Ring apophysis of the vertebra	Scheuermann	13–17
2 Iliac crest apophysis	Buchmann	
3 Pubic symphysis	Pierson	
4 Ischiopubic synchondrosis	Van Neck	4–11
5 Humeral head epiphysis	Hass	
6 Humeral capitellum	Panner	5–10
7 Metacarpal head	Dietrich/Mauclair	
8 Phalangeal base	Thiemann	11–19
9 Femoral head epiphysis	Legg-Calvé-Perthes	4–8
10 Patella	Sinding-Larsen	10–14
11 Medial tibial epiphysis	Blount	1–3 (infantile form) 8–15 (adolescent form)
12 Tibial apophysis	Osgood-Schlatter	11–15
13 Calcaneus apophysis	Sever	9–11
14 Navicular bone	Kohler I	3–7
15 Metatarsal head	Kohler II, Freiberg	13–18

Fig. 38.22 Localisation of juvenile osteochondrosis (for numbering, see **Table 38.5**)



■ ■ Imaging

Early changes of Perthes disease on conventional radiographs are:

- Displacement of the lateral capsular and iliopsoas fat pad
- Lateral displacement of the femoral ossification centre resulting in an enlargement of the medial joint space
- Smaller femoral ossification centre compared to the opposite side
- Subchondral fracture mostly of the anterolateral head segment (crescent sign)
- Intraepiphyseal gas
- Osteoporosis caused by inactivity

More **advanced stages** of this disease demonstrate the following radiographic features (**Fig. 38.23**):

- Metaphyseal cysts
- Diffuse femoral head thickening
- Femoral head fragmentation
- Widening and shortening of the femoral neck with disproportional larger greater trochanter; coxa vara
- Reparation stage with reformation of the femoral head
- Coxa magna and plana deformity (residual flattening and enlargement of the femoral head)

The course and severity of the disease are highly variable. The disease can completely heal but frequently a residual deformity,

coxa magna and plana, due to incomplete reconstitution of the femoral ossification centre can be identified. With the assessment of the extent of the epiphyseal necrosis the Catterall classification provides important information on the prognosis of the disease. While the prognosis of the disease in stages I and II are good or still good, prognosis becomes worse in stages III and IV (**Fig. 38.24**, overview).

Conventional radiographs, AP view and frog lateral view (Lauenstein view), are the basis for diagnostic imaging of Perthes disease.

In the event of negative radiographic findings, **MRI** is able to detect necrosis of the femoral head in its early stages. Necrosis appears with decreased signal in T1w and accompanying oedema in T2w images or STIR images. MRI enables an exact definition of the extension of the epiphyseal necrosis, and in unclear cases it can help determine the relationship to fragmentation and reparation stage. An early reparation stage is characterised by the occurrence of islands of fatty marrow in the femoral head.

Catterall classification of Perthes Disease

- **Stage I** solely involves a circumscribed anterior portion of the epiphysis. No fracture or collapse. No sequestrum. Metaphyseal changes unusual.



Fig. 38.23a,b Perthes disease. Radiological findings. **a** AP radiograph of the pelvis, **b** coronal PD w fat-suppressed image. The images demonstrate Perthes disease of the right hip in the fragmentation stage. Lateral displacement of the femoral ossification centre and metaphyseal cysts are visualised. Compared to the opposite side, shortening of the femoral neck, with disproportional larger greater trochanter and coxa vara are evident

- **Stage II** is characterised by affliction of larger portions of the anterior epiphysis. Fracture with formation of a sequestrum (sclerotic fragment). Intact bone medial and lateral to the sequestrum (maintaining epiphyseal height) in the AP view is seen
- When larger portions of the epiphysis are necrotic, with only small peripheral areas of uninvolved bones, the occurrence has reached **stage III**. Only a small, posterior portion of the head is uninvolved in the lateral view. Pronounced metaphyseal changes are usually seen.
- **Stage IV** involves the whole epiphysis. Early collapse of the epiphysis. Collapsed epiphysis appears as a dense line in the AP view. Extensive metaphyseal changes.

■ Scheuermann's Disease

■ ■ Definition

Synonyms: Adolescent kyphosis, Juvenile kyphosis.

Scheuermann's disease is regarded as a developmental disorder of the endplates of the vertebral bodies accompanied with deep thoracic kyphosis of different degrees of severity.

■ ■ Clinical Presentation

Adolescents between the ages of thirteen and seventeen are mostly affected. Clinical symptoms vary greatly. While some patients are without symptoms, others present with acute back pain and stiffening of the affected spinal segments. Scheuermann's disease predominantly occurs in the middle and lower thoracic spine (T4–T12); the frequency of isolated lumbar or cervical involvement is far less.

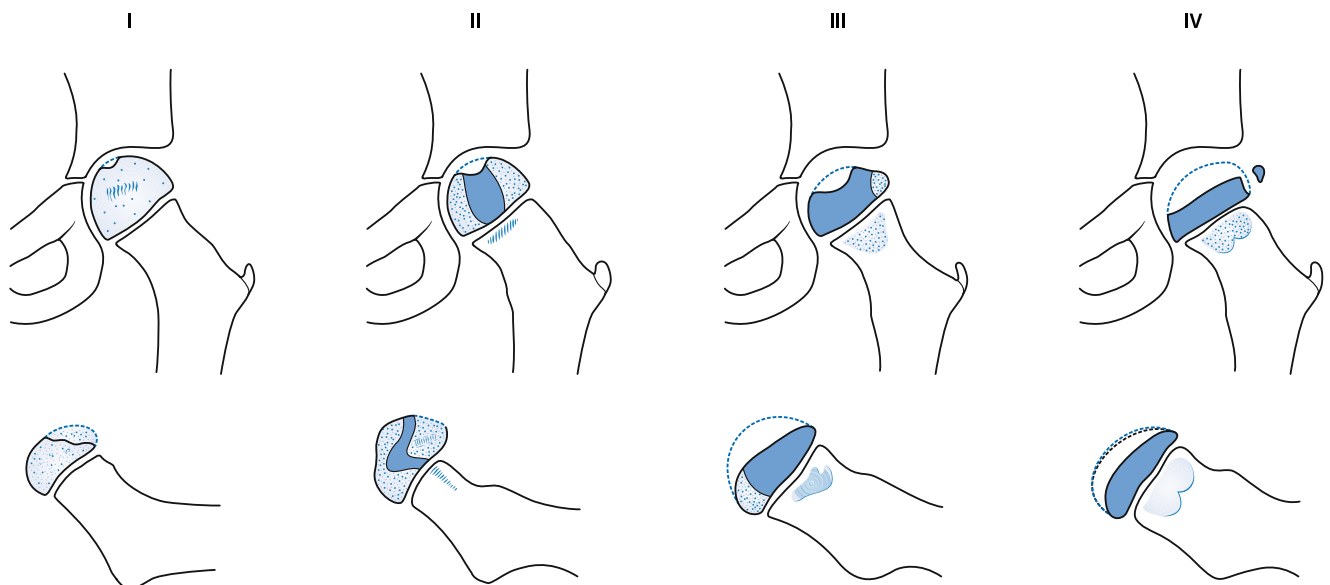
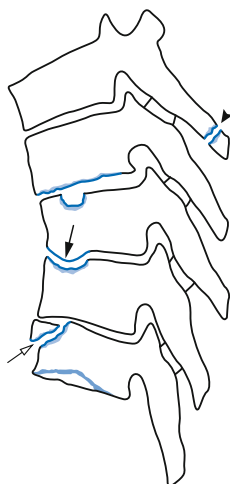


Fig. 38.24 Catterall stages of Perthes disease. For stages, see overview

■ **Fig. 38.25** Synopsis of the characteristic radiographic findings of Scheuermann's disease (after Dihlmann). *Top to bottom*: a wedge shaped deformity of the vertebral bodies, a marked decline of the intervertebral space ventrally, a enlarged vertebral body diameter, thickened endplates, Schmorl's nodes (typical in the ventral third), which partly leads to compensatory bone growth (Edgren–Vaino sign; *black arrow*), retromarginal disc prolapse (edge detachment; *arrow*), and possibly fatigue fractures in the area of the spinous processes (*arrowhead*)



■ ■ Imaging

The following features are characteristic of Scheuermann's disease in conventional imaging (■ Fig. 38.26):

- Convex anterior contour of vertebrae
- Wedge-shaped deformity of vertebral bodies with increased sagittal vertebral diameter in later stages
- Ventrally emphasised decrease of height of intervertebral space
- Contour irregularities of the endplates
- Intraspongious disc herniation (Schmorl nodes)
- Limbus vertebrae develops because of retromarginal cartilage prolapse between ring epiphysis and vertebrae
- Edgren–Vaino signs: compensatory bone growth causes osseous warp in base plate parallel to larger Schmorl nodes

38.4.3 Bone Infarction

■ ■ Definition, Aetiology

A bone infarct is a circumscribed necrosis of cancellous bone and bone marrow; the cortical bone is not affected. The cause of a bone infarct is a disruption or reduction of the blood supply. This can be triggered by the following diseases:

- Trauma
- Fractures or dislocations
- Changes in the vessels due to thrombosis or embolisms (e.g. sickle cell anaemia or other haemoglobinopathies)
- Vasculitic vessel damage (e.g. systemic lupus erythematosus)
- In increased pressure on the blood vessels through haemorrhages, fatty deposits in osteophytes

Many risk factors are known: cortisone or chemotherapy (e.g. methotrexate), Cushing's disease, alcohol abuse, Gaucher's disease, state after kidney transplantation, radiotherapy or Caisson's disease caused by nitrogen bubbles.

■ ■ Localisation, Clinical Presentation

Usually bone infarcts are located metaphyseally or metadiaphyseally in the long bones. They are less commonly located epiphyseally in the distal femur or the proximal tibia. Additionally, in exceptional cases, the proximal femur, the distal tibia or the proximal humerus may be affected.

The clinical manifestation of a bone infarct ranges from a completely asymptomatic picture, through persistent pain, up to sudden shooting pains, which are probably triggered by fractures of the cancellous bone.



■ **Fig. 38.26a–c** Scheuermann's disease. **Radiological findings.** a Radiograph of lumbar spine in lateral view demonstrates intraspongious cartilaginous hernia (Schmorl nodes) and contour irregularities of the endplates. In addition, ventral flattening at several vertebrae and enlarged sagittal diameter especially of the L4 are evident. b Sagittal T1w MRI reveals several

intraspongious cartilaginous hernias. At L3, across from the Schmorl node, a compensatory bone growth with mild osseous warping is evident (Edgren–Vaino sign). c Cross section of lumbar spine in lateral view demonstrates delineated retromarginal cartilage prolapse of L5

■ ■ Imaging

At the acute stage of the bone infarct no characteristic finding can be ascertained on **radiographs**. The affected bone may appear to have no distinctive features. However, diffuse demineralisation, patchy increases in lucency and lamellar periosteal reactions are also evident. At this stage, therefore, the differential diagnosis with regard to an inflammatory or tumourous process can be difficult. Later, very characteristic, indistinctly delineated lucency with a geographic pattern is shown, surrounded by a peripheral margin of sclerosis shaped like a garland (■ Fig. 38.27). In addition, a mature infarct can demonstrate secondary intralesional calcifications that originate in the fat tissue necrosis.

On nuclear medicine imaging the bone infarct initially appears as a “cold spot” as a sign of the reduced enhancement of the necrosis, whereas later on a higher uptake of Tc-^{99m} phosphonates (“cold in hot spot”) is observed.

On **MRI**, the older infarct has a very typical appearance (■ Fig. 38.27):

- A geographic area that is iso- or slightly hyperintense to normal fatty tissue on T1-weighted images is characteristic, surrounded like a garland by a hypointense margin.
- The border zone shows on T2- and contrast-enhanced T1-weighted fat-suppressed images a typical **double line sign**: consisting of a hypointense outer zone (reactive sclerosis) and a hyperintense inner zone (granulation tissue).
- In the area of necrosis secondary cystic degeneration and calcifications can occur.

38.5 Bone Changes in Diseases of Haematopoietic and Reticulohistiocytic Systems

K. Holzapfel

38.5.1 Anaemia

Anaemia is a decrease of haemoglobin concentrations in blood to <13.5 g/dl in men and 12 g/dl in women. There are many possible causes for anaemia, for example deficiency of iron, folic acid, or vitamin B12 as well as myeloproliferative diseases that cause haematopoietic suppression. Haemoglobinopathies, i.e., genetic defects of haemoglobin synthesis, are associated with bone changes visualised in radiologic imaging modalities. The quick decomposition (haemolysis) of functional inferior red blood cells causes secondary increased and quickened erythropoiesis that can be so pronounced that it leads to compensatory hyperplasia of blood-building bone marrow.

■ Haemoglobinopathies

■ ■ Sickle Cell Anaemia

Definition, Aetiology Sickle cell anaemia is the most common haemoglobinopathy. A point mutation creates a change of the amino acid sequence of the β-chain of haemoglobin and synthesis of abnormal haemoglobin molecules (HbS). A decrease of oxygen tension in blood leads to precipitation of HbS in hetero-

zygous people. Erythrocytes increase in sickle form, lose their plasticity, obstruct capillaries, and lead to organ infarction.

Clinical Presentation Organ infarctions occur as a so-called vaso-occlusive crisis. The vaso-occlusive crisis is usually experienced during childhood and is often accompanied with fever and abdominal pain. It tends to affect the spleen, lungs, heart, brain, and bones. Recurring splenic infarction can lead to functional asplenia and as a result demonstrate a noticeably elevated tendency for infection. Because of elevated haemolysis, gallstones develop (pigment stones).

The persistence of blood-building red bone marrow in the short long bones of infants and toddlers (1/2 year to 2 years of age) commonly leads to painful “hand-foot-syndrome” with symmetric swelling of fingers that are overly warm to touch.

Heterozygous persons usually do not show any symptoms but demonstrate resistance to the causative agents of malaria. This explains the common occurrence of mutation in Africa.

Imaging The following outlines changes and complications associated with sickle cell anaemia that affect bone as well as its characteristics in medical imaging:

■ Bone marrow hyperplasia:

Increased haematopoiesis leads to hyperplasia of bone marrow with new formation of red bone marrow from yellow fatty marrow. This reconversion develops from the centre to the periphery, therefore affecting first and foremost the spine, skull, pelvis, ribs, and in later stages the long bones. In the plain radiograph this development appears as osteopaenia with trabecular thickening, and thinning of the compacta. In long bones it leads to osseous distension with partially periosteal new bone formation (Erlenmeyer flask deformities of the distal femur). A characteristic at the calotte is the extension of diploë with initial narrowing of the external tabula and further narrowing of the internal tabula. The base of the occipital bone and facial bones remain unaffected (DD thalassaemia). The ribs demonstrate a slightly bulbous pronouncement. In MRI the substitute of yellow fatty marrow (hyperintense in T1w images) demonstrates a signal decrease in T1w images and a signal increase in T2w images. This signal change can be inhomogeneous and should not be confused with an infiltration of tumourous or infected cells. Extramedullary haematopoiesis is sometimes observed, for example in paravertebral soft tissue formation.

■ Bone infarction:

Vascular occlusion caused by malformed erythrocytes (which lead to osteonecrosis) occurs in bone, especially at the proximal and distal femur, proximal tibia and humerus, and the spine. An inhomogeneous image composed of patchy sclerosis and osteolysis appears in imaging studies. Subperiosteal new bone formation occurs parallel to linear cortical thickening in the diaphysis, which defines the characteristic image of “bone in bone.” The eventual fusion of these thickenings with cortical bone gradually leads to cortical thickening and to narrowing of the medullary space. In adults epiphyseal bone infarc-



Fig. 38.27a–c Bone infarction. Radiological findings. **a** AP radiograph shows characteristic polycystic or garland-shaped sclerotic zones that surround indistinctly defined increase in transparency. **b, c** On coronal STIR (**b**) and T1-weighted (**c**) images on fat-equivalent lesion is shown surrounded by

a garland-shaped margin. On the STIR image a border zone consists of a hypointense margin (outside) and a hyperintense portion (inside), the so-called “double line sign”

tion occurs first and foremost in the femoral and humeral head; its radiomorphology does not differ from osteonecrosis of other origin (► Sect. 38.4). In children, because of ischaemia of vertebral epiphysis, a slight central depression of endplates occurs, resulting in the characteristic H vertebrae of sickle cell anaemia. In children, small long bone infarction usually leads to painful dactylitis with inhomogeneous sclerosis and periostitis with periosteal new bone formation.

— Osteomyelitis/septic arthritis:

A weak immune system multiplies the incidence of bacterial osteomyelitis by 100. The most common cause (>50%) is *Salmonella* passed into the blood stream through intestinal ischaemia, followed by *Staphylococci*. The long bones are predominantly affected; facial bones and vertebrae are less commonly affected. Radiologic manifestation does not differentiate from osteomyelitis in patients without sickle cell anaemia (► Chap. 35). The same applies to septic arthritis. Articular effusion, soft tissue swelling, joint gap narrowing, and periarticular osteopaenia are determining findings.

■ ■ Thalassaemia

Definition, Aetiology Thalassaemia is a genetically determined disorder of haemoglobin synthesis. Mostly β haemoglobin chains

are not synthesised or have clearly decreased production (β Thalassaemia); the α haemoglobin chain occurs less frequently (α Thalassaemia). The degree of severity of thalassaemia is noticeably milder in heterozygous people (minor form) than in homozygous people (major form, synonym: Cooley anaemia).

Epidemiology, Clinical Presentation Thalassaemia shows the highest prevalence among people of the Mediterranean. Next to a high level of anaemia, clinical presentation includes the results of secondary organ haemosiderosis resulting from iron overload caused mostly by regular transfusion. Bone changes are prominent in the major form of β thalassaemia. Similar to sickle cell anaemia, these changes partially result from reactive bone marrow hyperplasia, which is especially pronounced in thalassaemia, also affects the facial bones, and frequently is associated with an extramedullary haematopoiesis. Compared to sickle cell anaemia, bone infarction is rare.

Imaging

— Bone marrow hyperplasia:

Similar to sickle cell anaemia, bone marrow hyperplasia leads to osteopaenia with cortical thinning and coarsening of trabecular structure, giving bone a striated appearance. In advanced osteoporosis, pathologic fractures may be

evident in especially the femur and lower arms. Osteoporosis of the spine appears through biconcave sinking of vertebral endplates, forming a fishbone appearance. As in sickle cell anaemia, distension of the distal femur in children leads to Erlenmeyer flask deformities. In the skull there is a widening of diploë space and formation of radial spiculae (hair-on-end appearance). Expansion of the maxilla can cause facial characteristics to appear coarsened. A malocclusion in the temporomandibular joint and a lateralisation of orbital caves are possible, giving the face a rat-like appearance. Osteolysis at the maxilla and mandibula lead to “floating teeth.” Widening of the nasal and temporal bones can sometimes lead to an obliteration of the nasal sinuses. Red bone marrow hernia through the anterior rib or extraosseous pedicle frequently causes extramedullary blood formation in paravertebral soft tissue formations.

■ Growth disruption/delayed bone maturation:

Irregular bands of sclerotic thickening at the ends of the long bones lead to bone retardation with dwarfism. Especially in the proximal humerus and distal femur, a premature closing of growth plates occurs. Because the closing of growth plates is frequently eccentric, varus deformities are common. Scoliosis is often observed in the spine.

■ Joint changes:

Repeated blood transfusions lead to secondary haemochromatosis with joint space narrowing and sclerotic changes in metacarpophalangeal joints as well as in the knee and hip. In addition, sometimes calcium pyrophosphate hydrate deposit (CPPD) crystals are observed in the meniscus and cartilage (pseudogout). Hyperuricaemia with consecutive gout is also possible. Treatment with iron chelates like deferoxamine can cause changes resembling rickets with distension of the metaphysis.

■ Other Types of Anaemia

■ Spherocytosis

Spherocytosis is the most common haemolytic anaemia in northern Europe. The genetically related defect of an erythrocyte membrane protein leads to formation of sphere-shaped red blood cells that are osmotically unstable. Radiologic changes are rare and are based on compensatory hyperplasia of haematopoietic bone marrow. Occurrence is predominant in the spine, in which case bone density decreases. Expansion of the diploë space and thinning of the external tabula is very rare.

■ Elliptocytosis

Similar to spherocytosis, a defect of erythrocyte membrane proteins causes this type of haemolytic anaemia. Skeletal changes are uncommon and correspond to those of spherocytosis (see above).

■ Iron Deficiency Anemia

Cases of pronounced iron deficiency may cause radial thickening of the skull.

■ Aplastic Anaemia

Aplastic anemia is an idiopathic disorder that arises following viral infection, medication, pregnancy, and other causes. It is defined by the formation of hypocellular bone marrow and the replacement of red bone marrow by yellow fatty marrow in the spine and pelvis as portrayed in T1w MRI by signal increase. Following therapy with erythropoietin, islands of blood-building marrow develop, creating a circumscribed signal loss in T1w images and signal increase in fat-suppressed images. For this reason, MRI is used for follow-up after beginning therapy.

38.5.2 Myeloproliferative Diseases and Leukaemias

Leukaemia is a family of diseases caused by diffuse, autonomic proliferation of degenerative leukopoietic cell clones. Different types of leukaemia are classified according to an acute or chronic course as per myeloid or lymphatic origin. Chronic myeloid leukaemia (CML) is categorised as a myeloproliferative disease, whereas chronic lymphatic leukaemia (CLL) is a form of mildly malignant Non-Hodgkin's lymphoma (NHL).

■ Acute Leukaemia

■ Acute Leukaemia in Childhood

Acute paediatric leukaemia occurs most frequently between the ages of two and five; it is mostly of lymphatic (ALL) origin and less so of myeloid (AML) origin. Osseous changes in acute leukaemia are more common in children (50–70%) than in adults (ca. 5%).

Imaging. A **diffuse osteopaenia** occurs first as the result of bone marrow infiltration by malignant cells. The medullary space appears widened and cortical bone appears narrowed. Pathologic fractures can occur. As a result of growth disruption, spinal osteopaenia can lead to stunted growth. Calcium salts also manifest in the skull as **granular atrophy** and later as larger osteolysis. Permeative osteolytic lesions may arise in advanced stages in the meta-/diaphysis of long bones, in particular in the medial proximal humerus metaphysis.

! Diffuse osteopaenia can precede the clinical manifestation of leukaemia by months!

A characteristic feature of acute leukaemia in childhood includes **horizontal, (sub)metaphyseal leukaemic lines** (Baty–Vogt lines); often accompanied by horizontal zones of sclerosis, these lines indicate temporary growth cessation. They develop symmetrically in the distal femur and proximal tibia and humerus. Predominantly diaphyseal, sometimes local **periosteal lesions** are evident, resulting in subperiosteal haemorrhaging or a leukemic cell infiltration. Probably resulting from elevated blood viscosity, **epiphyseal osteonecrosis** can lead to osteosclerotic thickening, especially in the femoral head. Note, bone infarction can also be related to therapy (glucocorticoid).

In cellular infiltration of synovia or interarticular bleeding, joint swelling, formation of joint effusion and periarticular osteopaenia occur. **Septic arthritis** occurs in affected joints.

Fig. 38.28a,b Acute myeloid leukaemia (AML) with chloroma. a AP radiograph of upper arm demonstrates poorly demarcated moth-eaten osteolytic lesion with destruction of cortical bone. b T1w MRI following contrast material administration demonstrates larger extraosseous tumour manifestations alongside bone marrow infiltration up to the epiphysis



■ Acute Leukaemia in Adults

Acute leukaemia in adults more frequently is of myeloid origin (AML). ALL can seldom emerge from CLL, and primary ALL in adults is rare. Osseous changes occur in adults with acute leukaemia in only approximately 5% of all cases.

Imaging. Diffuse osteopaenia is usually evident along with circumscribed osteolysis or sclerotic lesions. Acroosteolysis, periostitis, or diffuse osteosclerosis are very rare.

■ Chronic Leukaemia

Chronic leukaemia only occurs in adults. Osseous changes are rare compared to acute leukaemia.

Imaging. Diffuse osteopaenia is again prevalent, whereas circumscribed osteolysis is less common. Sclerotic lesions or periosteal changes are rare. Joint changes within the context of gout and septic arthritis can occur. The occurrence of **leukemic acropachy or dactylitis** during blast crisis is rare; these develop in soft tissue and demonstrate flask-shaped distension in metacarpals. Proliferic cell infiltration of bone marrow replacing fatty marrow generally demonstrates a loss of signal in T1 images and signal increase in fat-suppressed images. These signal changes can be diffuse (i.e., ALL) or focal (i.e., AML). Signal change is difficult to see in children, as children still possess peripheral blood-building marrow.

■ Special Forms of Leukaemia

■ Hairy Cell Leukaemia

Hairy cell leukaemia involves a low malignant NHL of B cells. The result of bone marrow fibrosis is a peripheral pancytopenia. Substantial splenomegaly with extensive lack of pronounced lymphadenopathy is common. The characteristic hairy cells possess thread-like cytoplasmic projections and show a positive re-

action to tartrate-resistant acid phosphatase. Men of middle to advanced age are mostly affected (75%).

Imaging. Radiologically, singular or multiple osteolysis appears in the spine or proximal femur.

■ Chloroma (Synonym: Granulocytic Sarcoma)

Chloroma defines a circumscribed, extramedullary accumulation of myeloblasts in both children and adults with AML. Children are more frequently affected.

Imaging. The soft tissue tumour can be solitary or multiple and can be infiltrative. In cases involving bone, pronounced osteolysis with periosteal reaction is evident. Soft tissue tumours may erode bone. The orbital bone, calotte, and long bones are the most common areas of occurrence (■ Fig. 38.28).

■ Polycythemia Vera

■ Definition, Epidemiology

Polycythemia vera is a myeloproliferative disease with autonomic proliferation of all three blood cell rows. It mostly affects older adults. Men are more frequently diagnosed than women and paediatric cases are very rare.

■ Clinical Presentation, Imaging

Clinical symptoms present as a form of plethora in which patients complain of pruritus, headache, dizziness, ringing in ears, epistaxis, and are often hypertonic. Thromboembolic complications are common. Bone changes are rare in adults but more common in children. The changes are a result of bone marrow hyperplasia and strongly resemble those in haemoglobinopathy (see above). **Osteolysis** is therefore a predominant finding, for example in the skull. Femoral head osteosclerosis is mostly the result of lo-

cal thrombosis. Generalised sclerosis is present during transition into osteomyelofibrosis. In the course of the disease, hyperuricaemia with consecutive gouty arthropathy is not uncommon.

■ Osteomyelofibrosis

■ Definition, Clinical Presentation

Osteomyelofibrosis is a myeloproliferative disease characterised by the following clinical triad:

- Marrow fibrosis with atrophy of blood-building bone marrow
- Extramedullary haematopoiesis (especially in the spleen and liver) with washout of immature precursor cells
- Splenomegaly

It can be primary or as a secondary occurrence to other myeloproliferative diseases. Aetiology is unclear.

■ Imaging

In radiologic examination, bone areas still possessing blood-building marrow demonstrate focal, spotted thickening of spongiosa, possibly distributed irregularly over the whole bone. The trabecular structure appears coarsened; an organisation in strain and compression lines is no longer recognisable. Thickening of cortical bone occurs and becomes increasingly difficult to differentiate from spongiosa. Bone contains a matted-glass aspect; the fine structure is no longer visible. Finally, the complete bone becomes sclerotic. Predilection sites are the vertebrae, pelvis, and ribs. Proximal long bones are affected in later stages. ■ Table 38.6 outlines common radiologic findings according to location.

MRI demonstrates signal loss in T1w images and in advanced fibrosis signal decrease in T2 sequences. As the result of characteristic expansion and permeability of medullary sinusoid, fat-suppressed STIR images can reveal a homogenous, hyperintense signal.

■ Systemic Mastocytosis

■ Definition

Systemic mastocytosis involves the systemic proliferation of mast cells. These gather in areas of bone in which blood-building marrow is present. Adults of middle age are affected.

■ Pathogenesis, Clinical Presentation

Resulting from histamine and serotonin release through mast cells, systemic mastocytosis involves a dysregulation of circulation and bowel function, flush, and urticaria pigmentosa. In addition, patients suffer reoccurring infection caused by pancytopenia and show an elevated tendency to bleed. Pronounced hepatosplenomegaly and lymph node swelling are common.

■ Imaging

Imaging studies reveal a clustering of osteolysis and spotted osteosclerosis in the spine and less frequently in the skull, pelvis, ribs, and proximal femur. Trabeculae appear thickened with washed-out contours. The ability to identify spongiosa and cortical bone becomes increasingly difficult. Changes can be focal or diffuse; bone demonstrates an ivory or chalky appearance. MRI portrays these areas as hypointense in T1w images and hyperin-

■ Table 38.6 Radiological manifestations of osteomyelofibrosis

Localisation	Radiological finding
Long bones	General changes (see above) Oval or moth-eaten, spotted osteolysis with indistinct delineation
Spine	Base and upper plate bands of sclerosis ("sandwich vertebral body sign")
Skull	Reduced delineation of diploë and tabula interna or externa
Mediastinum	Paravertebral soft-tissue formation (extramedullary haematopoiesis)
Joints	Periarticular sclerosis Joint space narrowing Subchondral erosions Haemarthrosis (consequence of impaired blood clotting) Sign of a gouty arthropathy

tense in T2w and STIR images. In advanced marrow sclerosis, T2w images also present a decrease in signal.

38.5.3 Diseases of Reticulohistiocytic Systems

■ Lipid Storage Disorder

Lipid storage disorder is a hereditary enzyme disorder resulting from disrupted lipid metabolism. It leads to an accumulation of complex lipids that deposit in tissue and macrophages and cells of the central nervous system.

■ Gaucher's Disease

Definition, Etiology, Epidemiology Gaucher's disease is an autosomal recessive hereditary disruption of glucocerebrosidase- β -glucosidase that causes glucosylceramides to collect in the reticuloendothelial system (spleen, liver, bone marrow). There are three subcategories for differentiation: a rare infantile form with cerebral involvement and very poor prognosis, a juvenile form, and a chronic form in adults without CNS involvement (most frequent). The disease is most prevalent among people of eastern European Jewish descent (Ashkenazy Jews).

Diagnosis, Imaging Bone changes are most common in chronic adult Gaucher's disease. The spine, pelvis, and long bones, in particular the distal femur, are the most frequent sites of infliction. By infiltration of lipid-storing macrophages, so-called Gaucher cells, the bone marrow becomes suppressed. Coarsening of spongiosa trabeculae, expansion of the medullary space with endosteal thinning of cortical bone, and general osteoporosis are evident.

Distension of the distal femur usually leads to **Erlenmeyer flask deformity**. Focal accumulations of Gaucher cells can create osteolytic patterns that resemble pseudotumours, bubbles, or a moth-eaten surface. Thinning of external and internal tabula occurs at the calotte. Findings in long bones often demonstrate a symmetric formation.

Osteoporosis leads to the frequent occurrence of pathologic fractures, especially at the spine, in which case the formation of an **H-form spine** (DD: sickle cell anemia) or **vertebra plana** can occur.

Because of compression of interosseous blood vessels by Gaucher cells, diaphyseal and epiphyseal osteonecrosis can develop, the latter being predisposed to arthritic changes. Diaphyseal infarction creates a “**bone in bone**” appearance by subperiosteal new bone formation parallel to cortical bone; this is also observed in haemoglobinopathy. The eventual fusion of these areas of cortical thickening gradually leads to thickening of the cortical bone. Osteomyelitis is common in Gaucher’s disease.

MRI is the method of choice for the imaging of bone marrow infiltration and bone infarction or osteomyelitis. Typical findings due to cellular changes of fatty marrow caused by Gaucher cells include signal loss in T1w and T2w images that can be homogenous or coarse and that initially do not affect the epiphysis. Acute osseous ischaemia, osteomyelitis, or oedema in occult fracture all appear with a signal increase in T2w images and in STIR sequences. MRI is also suitable for follow-up after beginning enzyme substitution therapy.

■ ■ Niemann–Pick Disease

Definition, Pathogenesis Niemann–Pick disease involves a family (with five subtypes) of rare, autosomal recessive hereditary diseases defined by a defect of sphingomyelin and cholesterol metabolism. The accumulating sphingomyelin metabolite is deposited in liver, spleen, bone marrow, and partially in the CNS.

Clinical Presentation Depending on its subtype, patients suffering from Niemann–Pick disease already show symptoms of neurologic disturbances in early childhood, are icteric in increased hepatosplenomegaly, or become blind (**cherry-red spot** of retina). Osseous changes resemble those of Gaucher’s disease. Foam cell infiltration into bone marrow leads to an expansion of the medullary space, thinning of cortical bone, and coarsening of spongiosa trabeculae. **Erlenmeyer flask deformities** can also be evident. Osteonecrosis, circumscribed osteolysis, or periosteal changes are not revealed. T1w MRI demonstrates a loss of signal due to fatty marrow replacement.

■ ■ Fabry Disease

Fabry disease is an extremely rare X chromosome recessive hereditary disorder of ceramide metabolism; therefore, men are predominantly affected.

Imaging. As bone changes, multiple osteonecroses, especially at the femoral head and talus, are prevalent. Acroosteolysis and productive fibroostosis are evident in the hands; the tendon sheath and joint capsules are usually thickened due to lipid deposits.

■ ■ Refsum Disease

Refsum disease is a rare disorder in which phytanic acid metabolism can cause ischaemic necrosis in the femoral head, shoulder, knee, hands, and feet. The metatarsals can demonstrate stunted growth.

■ Glycogen Storage Diseases

Osseous changes occur in some types of this heterogenous family of metabolic disorders that show increased deposits of glycogen. They arise in delayed bone maturation, general osteoporosis with expansion of medullary space, and coarsening of trabecular pattern. The metatarsals and phalanges are mostly affected. Gout commonly occurs as the result of pronounced hyperuricaemia.

■ Histiocytosis

■ ■ Langerhans Cell Histiocytosis

Eosinophilic granuloma, Hand–Schueller–Christian disease, and Abt–Letterer–Siwe disease – the three diseases involving Langerhans cell histiocytes, are referenced in another section (► Sect. 37.6).

■ ■ Multicentric Reticulohistiocytosis

This disease is also referenced in another chapter (► Sect. 39.1.6).

■ ■ Lipogranulomatosis (Erdheim–Chester Disease)

In this extremely rare disease of unknown aetiology, a granulomatous accumulation of lipid-storing histiocytes occurs in numerous sites, for example in the lungs, orbital bone, and retroperitoneal space.

Imaging. Osseous changes and their associated radiologic findings are characteristic. In the metaphysis and diaphysis of long bones, especially of the legs, a symmetric sclerosis mostly occurs which spares the epiphysis. Endosteal and periosteal new bone formation make it increasingly difficult to differentiate spongiosa and cortical bone. Osteolysis or spinal lipogranulomatosis are rare. In MRI, because of fatty marrow replacement, a signal decrease is seen in T1w images. Following administration of contrast agent, inhomogeneous enhancement is evident.

38.6 Systemic Osteoarthropathies

S. Waldt

38.6.1 Phakomatoses

Phakomatoses are hereditary neurocutaneous syndromes associated with dysplasia and neoplasms derived from the neuroectoderm and mesoderm.

The following conditions are categorized as phakomatoses:

- Neurofibromatosis
- Tuberous sclerosis
- Sturge–Weber syndrome
- Hippel–Lindau syndrome

Characteristic skeletal changes are seen in tuberous sclerosis and neurofibromatosis.

■ Tuberous Sclerosis

■ ■ Definition, Epidemiology, Etiology

Synonyms: Bourneville–Pringle disease, epiloia.

Tuberous sclerosis has a frequency of ca. 1:40,000. It is defined as a rare autosomal dominant hereditary syndrome with a

spontaneous mutation rate of 50–95%. It occurs without gender predilection and has an overall poor prognosis due to its progressive course.

■ ■ Clinical Presentation, Imaging

Tuberous sclerosis is characterised by a **triad of epileptic seizures, mental retardation, and skin lesions**.

Its occurrence includes the following:

- **Skin lesions:** adenoma sebaceum, periungual fibroma, hypopigmented macules
- **CNS lesions:** hamartoma: subependymal glial nodules, cortical tubers
- **Osseous lesions:** patchy or diffuse sclerosis that can be present in all parts of the skeleton, predilection sites: skull, pelvis, and lumbar spine
- Cortical lesions in the form of cystic lesions, sclerotic lesions and undulated periosteal reactions in the hand skeleton

■ Neurofibromatosis

■ ■ Definition, Epidemiology, Etiology

Neurofibromatosis has an incidence of 1:3,000. It is a relatively common hereditary condition; women and men are equally affected. Eight subgroups have been identified up until today; neurofibromatosis type 1 (Recklinghausen disease) and type 2 (central neurofibromatosis) are the most common of all subgroups.

■ ■ Clinical Presentation, Imaging

Whereas neurofibromatosis type 1 characteristically demonstrates intracerebral and intraspinal tumours of glial and neuronal genesis, neurofibromatosis type 2 typically demonstrates neoplastic lesions caused by Schwann cells, the meninges, or the ependyma. Bilateral acoustic neuroma is especially characteristic of neurofibromatosis type 2. Compared with the occurrence of neoplasm, skin lesions and osseous lesions recede into the background in neurofibromatosis type 2, these changes are characteristic signs of neurofibromatosis type 1 (► Sect. 9.2).

The following findings are common for **neurofibromatosis type 1 (Recklinghausen disease)**:

- **Skin lesions:** café-au-lait spots, molluscum fibrosum, skin tumours: neurofibroma, plexiform neurofibroma, schwannoma
- **Intracerebral tumours:** optic pathway glioma, diencephalic glioma, brainstem glioma
- **Eye manifestations:** iris hamartoma (Lisch nodules)
- **Osseous manifestations:**
 - **Skull:** sphenoid wing dysplasia
 - **Spine:** angular kyphoscoliosis, vertebral dysplasia; expansion of neuroforamina through schwannoma, flattening of vertebral arches by intramedullary tumours; dura ectasia leads to scalloping of the posterior vertebral bodies
 - **Long bones:** dysplasia of long bones: bowing, pathologic fractures, pseudarthrosis due to an abnormally poor bone structure

■ Sturge–Weber Syndrome

■ ■ Definition, Clinical Presentation

Synonyms: Encephalotrigeminal syndrome, Sturge–Weber–Krabbe syndrome, encephalotrigeminal angiomas.

In this syndrome the leading finding is a capillary-venous angiomas that affects the vessels of the facial skin (the supply area of the trigeminal nerve), the leptomeninges, and of the eye. The following clinical symptoms are present: nevus flammeus, seizure, mental retardation, ipsilateral glaucoma, and hemiparesis.

■ ■ Imaging

Radiograph of the skull typically portrays tram track calcifications caused by calcifications of leptomeningeal vessels.

38.6.2 Amyloidosis

■ ■ Definition

Amyloidosis is a group of diseases characterised by localised or generalised deposits of amyloid in various organs. Amyloid involves a heterogeneous glycoprotein with β -sheet structure interstitially deposited.

Alongside primary amyloidosis the following diseases can lead to **secondary amyloidosis**:

- Malignant monoclonal gammopathy (plasmacytoma)
- Chronic haemodialysis (β_2 microglobulin deposits in 65% of patients after 10-years of dialysis)
- Chronic inflammatory diseases, for example rheumatoid arthritis, seronegative spondyloarthropathy, and Crohn's disease

■ ■ Pathogenesis, Clinical Presentation

Amyloid osteoarthropathy is characterised by deposits in the synovial membrane, articular cartilage, periarticular soft tissue, and juxtacortical bone. Clinical symptoms include limitation of motion, nightly joint pain, and partially elevated soft tissue swelling.

■ ■ Imaging

The following describe characteristic imaging features of amyloidosis:

- **Wrist (capitate, lunate, and scaphoid), proximal femur, and proximal humerus:** “cystoid” (smoothly marginated, subchondral location) lesions, partially with discrete sclerotic rim
- Large joints (**shoulder and hip joint**) usually present a bilateral symmetric occurrence; the joint space is typically of normal width but sometimes enlarged due to amyloid deposits; soft tissue swelling is characteristic
- **Bursae** (e.g., olecranon bursa, subacromial bursa): elevated swelling of bursae is sometimes present, sometimes with erosive changes of the adjacent bones

► **It is typical for amyloid deposits to demonstrate low signal intensity on T1w and T2w MR images.**

38.6.3 Sarcoidosis

■ ■ Definition, Aetiology, Epidemiology

Synonym: Boeck disease.

Sarcoidosis is a granulomatous systemic disease of unclear aetiology that manifests first and foremost in the lungs and in other organs as well (► Sect. 19.8.6). Peak age lies between the second and fourth decade of life, and women are affected more frequently than men.

An involvement of the skeletal system is observed in 5–15% of cases, especially in the chronic long-term course of the disease. Noncaseating epithelioid cell granulomas may occur in the bone marrow cavity and in the synovial membrane. This leads to inflammatory reactions in the synovial membrane. The most common sites of articular involvement are the knee, ankle, and elbow. Osseous involvement is typical in the phalanges of the hand, referred to as *ostitis cystoides multiplex Jüngling*. Osseous occurrences in the skull, thoracic and lumbar spine, and pelvis are rare.

■ ■ Clinical Presentation

Next to acute polyarthritis, clinical symptoms in joint involvement can also include chronic swelling and pain. An acute course of sarcoidosis, known as Löfgren syndrome, is characterised by fever, polyarthralgia, erythema nodosum, and iritis. The most commonly affected joints are the knee and ankle, both symmetrically. Histologically, in acute form, nonspecific synovitis without granulomatous changes are characteristic. The osseous involvement is often asymptomatic.

■ ■ Imaging

The following radiographic features in the **phalanges** are typical (■ Fig. 38.29):

- Epimetaphyseal, well-demarcated, small round or oval osteolytic lesions only a few millimetres in size, with or without a sclerotic rim
- A coarse trabecular pattern next to cystic areas
- Honeycomb pattern of bone structure
- Acroosteolyses
- Periosteal (undulated) reactions

Bibliography

References

- Barnett E, Nordin B. The radiological diagnosis of osteoporosis: a new approach. *Clin Radiol* 1960;11:166–174
- Genant HK, Wu CY, van Kuijk C, Nevitt MC. Vertebral fracture assessment using a semiquantitative technique. *J Bone Miner Res* 1993;8:1137–1148
- Meunier P, Bressot C, Vignon E, Edouard C, Alexandre C, Coupron P et al., Radiological and histological evolution of post-menopausal osteoporosis treated with sodium fluoride-vitamin D-calcium. Preliminary results. Bern: Hans Huber Publishers, 1978
- Minne H, Leidig G, Wüster C, et al. A newly developed spine deformity index (SDI) to quantitate vertebral crush fractures in patients with osteoporosis. *Bone Miner* 1988;3:335–349



■ Fig. 38.29 Multiple cystic tuberculous skeletal lesions or *Jüngling* disease. Sarcoidosis of the phalanges. AP radiograph of the forefoot demonstrates osseous changes of the phalanges: proximal and distal phalanx D1, distal phalanx D2, and proximal phalanx D4. Next to well-demarcated cystoid lesions in epimetaphyseal location (D1 and D4), a restructuring of bone of proximal and distal phalanx D5 with increased honeycombed trabecular pattern is evident

Further Reading

- Albright F, Burnett C, Smith P, Parson W. Pseudohypoparathyroidism – an example of Seabright–Bantam syndrome. *Endocrinology* 1942;30:922
- Bogost G, Liserbram E, Crues J. MR imaging in evaluation of suspected hip fracture: frequency of unsuspected bone and soft-tissue injury. *Radiology* 1995;197:263–267
- Cann C, Genant H, Kolb F, Ettinger B. Quantitative computed tomography for the prediction of vertebral body fracture risk. *Bone* 1985;6:1–7
- Cummings S, Nevitt N, Browner W. Risk factors for hip fracture in white women. Study of Osteoporotic Fractures Research Group. *N Engl J Med* 1995;332:767–763
- Delling G. Neuere Vorstellungen zu Bau und Struktur der menschlichen Spongiosa-Ergebnisse einer zwei- und dreidimensionalen Analyse. *Z gesamt inn Med* 1989;44:536–540
- Felsenberg D, Gowin W. Knochendichtemessung mit Zwei-Spektren-Methoden. *Radiologie* 1999;39:186–193
- Häussler B, Goethe H, Mangiapane S, Glaeske G, Podsiadlo P, Felsenberg D. Versorgung von Osteoporose-Patienten in Deutschland, Ergebnisse der Bone EVA-Studie. *Deutsches Ärzteblatt* 2006;103(39):2542–2548

- Heuck F. Qualitative und quantitative radiologische Analyse des Knochens. In: Schinz H (ed). *Radiologische Diagnostik in Klinik und Praxis*. Stuttgart, New York: Georg Thieme Verlag 1989
- Leidig-Bruckner G, Genant HK, Minne HW, et al., Comparison of a semiquantitative and a quantitative method for assessing vertebral fractures in osteoporosis. *Bone* 1994;15(4):437–442
- Mayet W, Hermann E, Wandel E, et al., Rheumatologische und radiologische Symptome bei sekundärem Hyperparathyreoidismus: Retrospektive Langzeit-Studie bei 175 chronischen Dialysepatienten. *Z Rheumatol* 1991;50:313–319
- Parfitt AM. Trabecular bone architecture in the pathogenesis and prevention of fracture. *Am J Med* 1987;82(suppl.1B):68–72
- Pfeilschifter J. 2006 DVO-guideline for prevention, diagnosis, and therapy of osteoporosis for women after menopause, for men after age 60 executive summary guidelines. *Exp Clin Endocrinol Diabetes* 2006;114(10):611–622
- Prevrhal S, Genant H. Quantitative Computertomographie. *Radiologe* 1999;39:194–202
- Schulz G, Manns M. Ätiologie, Diagnostik und Therapie der Osteoporose. In: Schild HH, Heller M: *Osteoporose*. Stuttgart: Thieme-Verlag 1992:27–51
- Tigges S, Nance E, Carpenter W, Erb R. Renal osteodystrophy: imaging findings that mimic those of other diseases. *Am J Roentgenol* 1995;165:143–150